



# TECH BRIEFS

NATIONAL AERONAUTICS AND SPACE ADMINISTRATION

-  **Technology Focus**
-  **Computers/Electronics**
-  **Software**
-  **Materials**
-  **Mechanics**
-  **Machinery/Automation**
-  **Manufacturing**
-  **Bio-Medical**
-  **Physical Sciences**
-  **Information Sciences**
-  **Books and Reports**



# INTRODUCTION

Tech Briefs are short announcements of innovations originating from research and development activities of the National Aeronautics and Space Administration. They emphasize information considered likely to be transferable across industrial, regional, or disciplinary lines and are issued to encourage commercial application.

## Availability of NASA Tech Briefs and TSPs

Requests for individual Tech Briefs or for Technical Support Packages (TSPs) announced herein should be addressed to

### National Technology Transfer Center

Telephone No. (800) 678-6882 or via World Wide Web at [www2.nttc.edu/leads/](http://www2.nttc.edu/leads/)

Please reference the control numbers appearing at the end of each Tech Brief. Information on NASA's Commercial Technology Team, its documents, and services is also available at the same facility or on the World Wide Web at [www.nctn.hq.nasa.gov](http://www.nctn.hq.nasa.gov).

Commercial Technology Offices and Patent Counsels are located at NASA field centers to provide technology-transfer access to industrial users. Inquiries can be made by contacting NASA field centers and program offices listed below.

## NASA Field Centers and Program Offices

### Ames Research Center

Carolina Blake  
(650) 604-1754  
[carolina.m.blake@nasa.gov](mailto:carolina.m.blake@nasa.gov)

### Dryden Flight Research Center

Gregory Poteat  
(661) 276-3872  
[greg.poteat@dfrc.nasa.gov](mailto:greg.poteat@dfrc.nasa.gov)

### Goddard Space Flight Center

Nona Cheeks  
(301) 286-5810  
[Nona.K.Cheeks.1@gsfc.nasa.gov](mailto:Nona.K.Cheeks.1@gsfc.nasa.gov)

### Jet Propulsion Laboratory

Art Murphy, Jr.  
(818) 354-3480  
[arthur.j.murphy-jr@jpl.nasa.gov](mailto:arthur.j.murphy-jr@jpl.nasa.gov)

### Johnson Space Center

Charlene E. Gilbert  
(281) 483-3809  
[commercialization@jsc.nasa.gov](mailto:commercialization@jsc.nasa.gov)

### Kennedy Space Center

Jim Aliberti  
(321) 867-6224  
[Jim.Aliberti-1@ksc.nasa.gov](mailto:Jim.Aliberti-1@ksc.nasa.gov)

### Langley Research Center

Jesse Midgett  
(757) 864-3936  
[jesse.c.midgett@nasa.gov](mailto:jesse.c.midgett@nasa.gov)

### John H. Glenn Research Center at Lewis Field

Larry Viterna  
(216) 433-3484  
[cto@grc.nasa.gov](mailto:cto@grc.nasa.gov)

### Marshall Space Flight Center

Vernotto McMillan  
(256) 544-2615  
[vernotto.mcmillan@msfc.nasa.gov](mailto:vernotto.mcmillan@msfc.nasa.gov)

### Stennis Space Center

Robert Bruce  
(228) 688-1929  
[robert.c.bruce@nasa.gov](mailto:robert.c.bruce@nasa.gov)

### NASA Program Offices

At NASA Headquarters there are seven major program offices that develop and oversee technology projects of potential interest to industry:

#### Carl Ray

Small Business Innovation Research Program (SBIR) & Small Business Technology Transfer Program (STTR)  
(202) 358-4652 or  
[cray@mail.hq.nasa.gov](mailto:cray@mail.hq.nasa.gov)

#### Benjamin Neumann

Innovative Technology Transfer Partnerships (Code RP)  
(202) 358-2320  
[benjamin.j.neumann@nasa.gov](mailto:benjamin.j.neumann@nasa.gov)

#### John Mankins

Office of Space Flight (Code MP)  
(202) 358-4659 or  
[jmankins@mail.hq.nasa.gov](mailto:jmankins@mail.hq.nasa.gov)

#### Terry Hertz

Office of Aero-Space Technology (Code RS)  
(202) 358-4636 or  
[thertz@mail.hq.nasa.gov](mailto:thertz@mail.hq.nasa.gov)

#### Glen Mucklow

Office of Space Sciences (Code SM)  
(202) 358-2235 or  
[gmucklow@mail.hq.nasa.gov](mailto:gmucklow@mail.hq.nasa.gov)

#### Roger Crouch

Office of Microgravity Science Applications (Code U)  
(202) 358-0689 or  
[rcrouch@hq.nasa.gov](mailto:rcrouch@hq.nasa.gov)

#### Granville Paules

Office of Mission to Planet Earth (Code Y)  
(202) 358-0706 or  
[gpaules@mtpe.hq.nasa.gov](mailto:gpaules@mtpe.hq.nasa.gov)





# TECH BRIEFS

NATIONAL AERONAUTICS AND SPACE ADMINISTRATION



## 5 Technology Focus: Data Acquisition

- 5 Data Relay Board With Protocol for High-Speed, Free-Space Optical Communications
- 6 Software and Algorithms for Biomedical Image Data Processing and Visualization
- 7 Rapid Chemometric Filtering of Spectral Data
- 8 Prioritizing Scientific Data for Transmission
- 8 Determining Sizes of Particles in a Flow From DPIV Data
- 9 Faster Processing for Inverting GPS Occultation Data



## 11 Electronics/Computers

- 11 FPGA-Based, Self-Checking, Fault-Tolerant Computers
- 12 Ultralow-Power Digital Correlator for Microwave Polarimetry
- 12 Grounding Headphones for Protection Against ESD
- 13 Lightweight Stacks of Direct Methanol Fuel Cells
- 14 Highly Efficient Vector-Inversion Pulse Generators



## 15 Software

- 15 Estimating Basic Preliminary Design Performances of Aerospace Vehicles
- 15 Framework for Development of Object-Oriented Software
- 15 Analyzing Spacecraft Telecommunication Systems
- 15 Collaborative Planning of Robotic Exploration
- 16 Tools for Administration of a UNIX-Based Network
- 16 Preparing and Analyzing Iced Airfoils
- 16 Evaluating Performance of Components



## 17 Materials

- 17 Fuels Containing Methane or Natural Gas in Solution

- 17 Direct Electrolytic Deposition of Mats of  $Mn_xO_y$  Nanowires



## 19 Mechanics

- 19 Bubble Eliminator Based on Centrifugal Flow
- 19 Inflatable Emergency Atmospheric-Entry Vehicles
- 20 Lightweight Deployable Mirrors With Tensegrity Supports



## 23 Machinery/Automation

- 23 Centrifugal Adsorption Cartridge System
- 23 Ultrasonic Apparatus for Pulverizing Brittle Material



## 25 Bio-Medical

- 25 Transplanting Retinal Cells Using Bucky Paper for Support
- 26 Using an Ultrasonic Instrument to Size Extravascular Bubbles



## 27 Physical Sciences

- 27 Coronagraphic Notch Filter for Raman Spectroscopy
- 28 On-the-Fly Mapping for Calibrating Directional Antennas
- 29 Working Fluids for Increasing Capacities of Heat Pipes



## 31 Information Sciences

- 31 Computationally-Efficient Minimum-Time Aircraft Routes in the Presence of Winds



## 33 Books & Reports

- 33 Liquid-Metal-Fed Pulsed Plasma Thrusters
- 33 Personal Radiation Protection System
- 33 Attitude Control for a Solar-Sail Spacecraft

This document was prepared under the sponsorship of the National Aeronautics and Space Administration. Neither the United States Government nor any person acting on behalf of the United States Government assumes any liability resulting from the use of the information contained in this document, or warrants that such use will be free from privately owned rights.





## Data Relay Board With Protocol for High-Speed, Free-Space Optical Communications

A fade-tolerant data relay system is proposed to ensure reliable delivery of data across an optical channel.

NASA's Jet Propulsion Laboratory, Pasadena, California

In a free-space optical communication system, the mitigation of transient outages through the incorporation of error-control methods is of particular concern, the outages being caused by scintillation fades and obscurants. The focus of this innovative technology is the development of a data relay system for a reliable high-data-rate free-space-based optical-transport network. The data relay boards will establish the link, maintain synchronous connection, group the data into frames, and provide for automatic retransmission (ARQ) of lost or erred frames. A certain Quality of Service (QoS) can then be ensured, compatible with the required data rate. The protocol to be used by the data relay system is based on the draft CCSDS standard data-link protocol "Proximity-1," selected by orbiters to multiple lander assets in the Mars network, for example. In addition to providing data-link protocol capabilities for the free-space optical link and buffering the data, the data relay system will interface directly with user applications over Gigabit Ethernet and/or with high-speed storage resources via Fibre Chan-

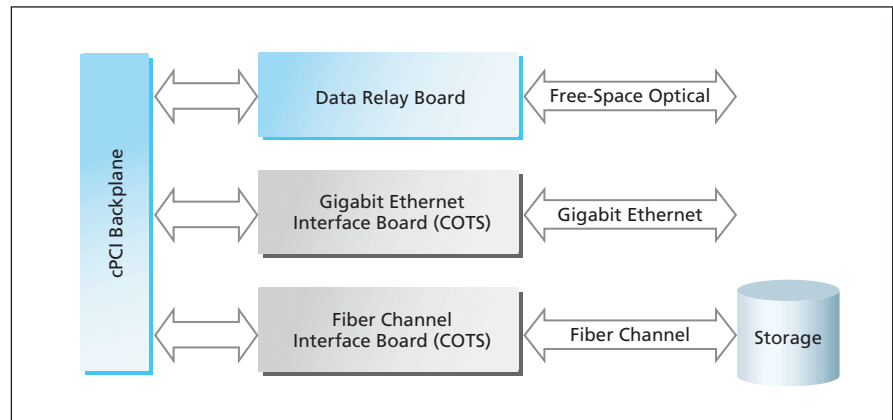


Figure 1. The Data Relay System block diagram shows the interfaces.

nel. The hardware implementation is built on a network-processor-based architecture. This technology combines the power of a hardware switch capable of data switching and packet routing at Gbps rates, with the flexibility of a software-driven processor that can host highly adaptive and reconfigurable protocols used, for example, in wireless local-area networks (LANs).

The system will be implemented in a modular multi-board fashion. The

main hardware elements of the data relay system are the new data relay board developed by Rockwell Scientific, a COTS Gigabit Ethernet board for user interface, and a COTS Fibre Channel board that connects to local storage. The boards reside in a cPCI back plane, and can be housed in a VME-type enclosure.

A block diagram of the data relay system is shown in Figure 1. The data relay board, shown in Figure 2, controls the

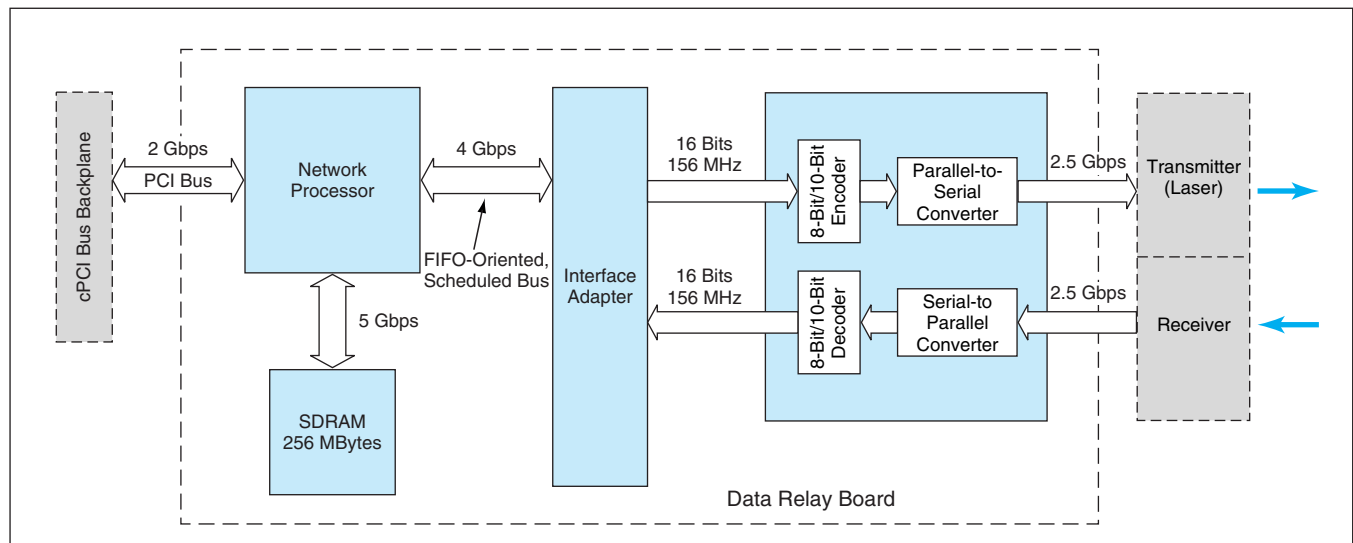


Figure 2. A Data Relay Board would be installed in a free-space optical communication terminal to ensure a reliable high-speed data link. The board would regulate the flow of data between the user application and the optical transceiver.

data flow between the cPCI bus on the one hand and the transmitter and receiver on the other hand once the free-space optical link has been established. The data rates in transmission and reception need not be equal and could even differ by as much as several orders of magnitude. The data relay board would contain a commercially available network processor programmed to perform the primitive data handling function required by the protocol. Using a memory buffer, the network processor would accept, from the user application or storage through the cPCI bus, a stream of data to be transmitted to the laser. The network processor would form the data into appropriately sized frames with headers and frame sequence information to identify frames for the ARQ process. The frames would then be sent to an interface adaptor for frame acquisition and synchronization.

The interface adaptor would then format the data into 16-bit words, add error check bits, and send the data to the serializer and encoder for transmission to the laser.

As successful receipt of frames is acknowledged using the free-space optical link in the reverse direction, the corresponding data are cleared from the local memory so that capacity for new streaming data is made available. In the event of missed or corrupted data frames, the network processor will reconstruct and retransmit the data frames over the free-space optical link.

On the receiving side, the interface adapter will check for errors, while the network processor will check for frames out of sequence. For each received frame, the network processor will generate the appropriate ARQ control frame and pass it to the reverse channel

free-space optical-link interface for transmission.

*This work was done by Malcolm Wright and Loren Clare of Caltech and Gary Gould and Maxim Pedyash of Rockwell Scientific Center for NASA's Jet Propulsion Laboratory. Further information is contained in a TSP (see page 1).*

*In accordance with Public Law 96-517, the contractor has elected to retain title to this invention. Inquiries concerning rights for its commercial use should be addressed to*

*Innovative Technology Assets Management  
JPL*

*Mail Stop 202-233*

*4800 Oak Grove Drive*

*Pasadena, CA 91109-8099*

*(818) 354-2240*

*E-mail: iaoffice@jpl.nasa.gov*

*Refer to NPO-30610, volume and number of this NASA Tech Briefs issue, and the page number.*

## Software and Algorithms for Biomedical Image Data Processing and Visualization

### PlaqTrak automatically assesses plaque deposits on teeth.

NASA's Jet Propulsion Laboratory, Pasadena, California

A new software equipped with novel image processing algorithms and graphical-user-interface (GUI) tools has been designed for automated analysis and processing of large amounts of biomedical image data. The software, called PlaqTrak, has been specifically used for analysis

of plaque on teeth of patients. New algorithms have been developed and implemented to segment teeth of interest from surrounding gum, and a real-time image-based morphing procedure is used to automatically overlay a grid onto each segmented tooth. Pattern recognition

methods are used to classify plaque from surrounding gum and enamel, while ignoring glare effects due to the reflection of camera light and ambient light from enamel regions. The PlaqTrak system integrates these components into a single software suite with an easy-to-use

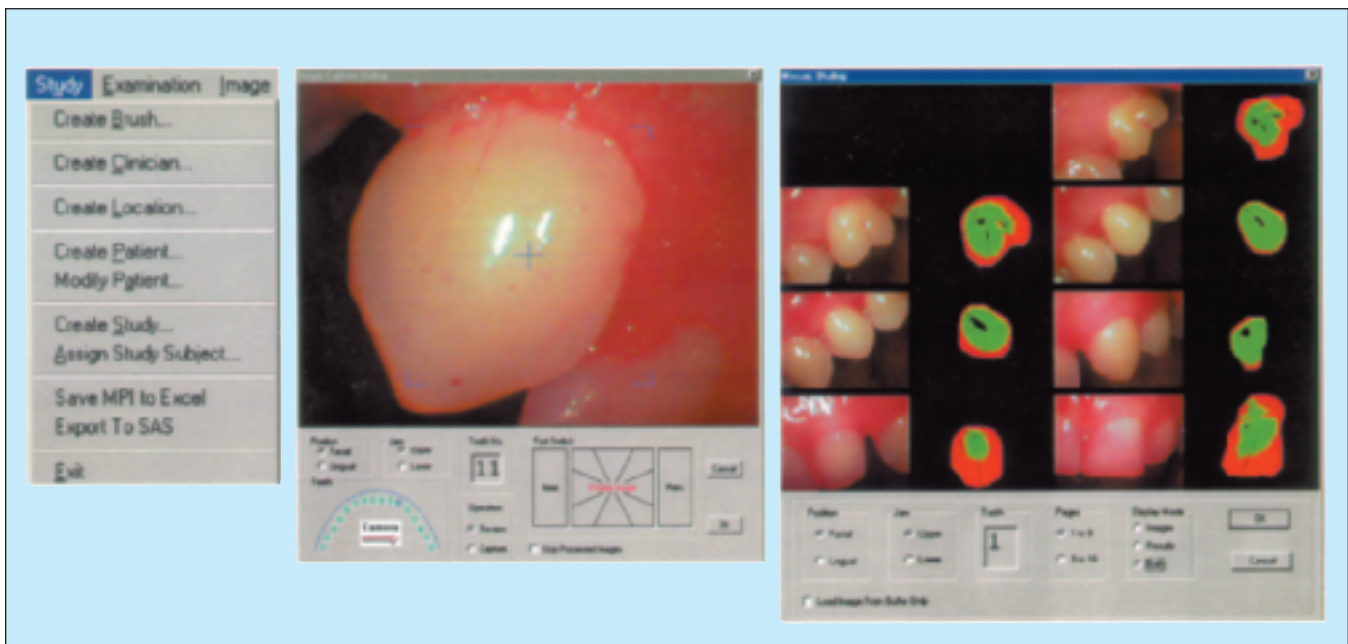


Figure 1. PlaqTrak System Utilities are showing some of the GUI tools.

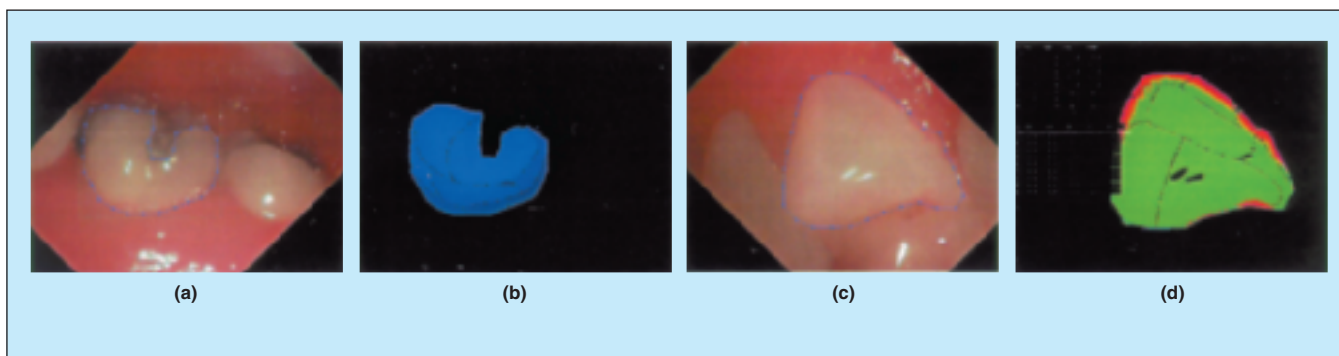


Figure 2. Examples are shown of **Biomedical Image** segmentation, morphing, and classification.

GUI (see Figure 1) that allows users to do an end-to-end run of a patient's record, including tooth segmentation of all teeth, grid morphing of each segmented tooth, and plaque classification of each tooth image.

The automated and accurate processing of the captured images to segment each tooth [see Figure 2(a)] and then detect plaque on a tooth-by-tooth basis is a critical component of the PlaqTrak system to do clinical trials and analysis with minimal human intervention. These features offer distinct advantages over other competing systems that analyze groups of teeth or synthetic teeth. PlaqTrak divides each segmented tooth into eight regions

using an advanced graphics morphing procedure [see results on a chipped tooth in Figure 2(b)], and a pattern recognition classifier is then used to locate plaque [red regions in Figure 2(d)] and enamel regions. The morphing allows analysis within regions of teeth, thereby facilitating detailed statistical analysis such as the amount of plaque present on the biting surfaces on teeth.

This software system is applicable to a host of biomedical applications, such as cell analysis and life detection, or robotic applications, such as product inspection or assembly of parts in space and industry.

*This work was done by Ashit Talukder, James Lambert, and Raymond Lam of Cal-*

*tech for NASA's Jet Propulsion Laboratory. Further information is contained in a TSP (see page 1).*

*In accordance with Public Law 96-517, the contractor has elected to retain title to this invention. Inquiries concerning rights for its commercial use should be addressed to:*

*Intellectual Assets Office*

*JPL*

*Mail Stop 202-233*

*4800 Oak Grove Drive*

*Pasadena, CA 91109*

*(818) 354-2240*

*E-mail: ipgroup@jpl.nasa.gov*

*Refer to NPO-30417, volume and number of this NASA Tech Briefs issue, and the page number.*

## **Rapid Chemometric Filtering of Spectral Data**

**Target species would be identified in real time.**

*NASA's Jet Propulsion Laboratory, Pasadena, California*

A method of rapid, programmable filtering of spectral transmittance, reflectance, or fluorescence data to measure the concentrations of chemical species has been proposed. By "programmable" is meant that a variety of spectral analyses can readily be performed and modified in software, firmware, and/or electronic hardware, without need to change optical filters or other optical hardware of the associated spectrometers. The method is intended to enable real-time identification of single or multiple target chemical species in applications that involve high-throughput screening of multiple samples. Examples of such applications include (but are not limited to) combinatorial chemistry, flow cytometry, bead assays, testing drugs, remote sensing, and identification of targets.

The basic concept of the proposed method is to perform real-time cross-

correlations of a measured spectrum with one or more analytical function(s) of wavelength that could be, for example, the known spectra of target species. Assuming that measured spectral intensities are proportional to concentrations of target species plus background spectral intensities, then after subtraction of background levels, it should be possible to determine target-species concentrations from cross-correlation values. Of course, the problem of determining the concentrations is more complex when spectra of different species overlap, but the problem can be solved by use of multiple analytical functions in combination with computational techniques that have been developed previously for analyses of this type.

The method is applicable to the design and operation of a spectrometer in which spectrally dispersed light is mea-

sured by means of an active-pixel sensor (APS) array. The row or column dimension of such an array is generally chosen to be aligned along the spectral-dispersion dimension, so that each pixel intercepts light in a narrow spectral band centered on a wavelength that is a known function of the pixel position. The proposed method admits of two hardware implementations for computing cross-correlations in real time.

One hardware implementation would exploit programmable circuitry within each pixel of an APS array. The analog spectral-intensity reading of the photodetector in each pixel would be multiplied by a gain proportional to value of the analytical function for the wavelength that corresponds to the pixel position. As a result, the output from each pixel would be proportional to contribution of the pixel to the cross-correlation (plus background). The outputs of

all the pixels along the spectral-dispersion dimension would be summed to obtain the value of the cross-correlation (plus background).

Such on-chip cross-correlation could be performed rapidly because the analytical function could be statically programmed into the APS array and the multiplications could be done simultaneously or nearly so. All of the additions could be done simultaneously by means of a single binning instruction. The charge wells of all the pixels could be connected simultaneously, collecting all the charge outputs from multiplication operations into one "super-pixel," the single readout value of which would constitute the cross-correlation value for the given analytical function. For an instrument in which the APS rows were aligned along the spectral-dispersion dimension and in which the image of a spectrograph slit was aligned along the pixel columns and spanned multiple pixel rows, it

would be possible to perform simultaneous cross-correlations for multiple target species by applying, to each pixel row, the analytical function corresponding to one of the target species. A separate readout would be needed for each target species.

In the other hardware implementation, cross-correlations would be computed externally to the APS array. The multiplications and additions would be performed in pipeline fashion. If the APS-array outputs were analog, then programmable analog signals representing the analytical functions would be synthesized in phase with the corresponding stream of analog APS-array outputs and the multiplications and additions would be performed by relatively inexpensive, commercially available analog mixing and filtering circuits, respectively. If the APS-array outputs were digital, the cross-correlations could be computed by a digital signal processor. Ordinarily, the analog

approach would be preferable because the analog operations can be performed much more rapidly than can the corresponding digital multiplications and additions.

*This work was done by Gregory Bearman, Michael Pelletier, and Suresh Seshadri of Caltech for NASA's Jet Propulsion Laboratory. Further information is contained in a TSP (see page 1).*

*In accordance with Public Law 96-517, the contractor has elected to retain title to this invention. Inquiries concerning rights for its commercial use should be addressed to:*

*Innovative Technology Assets Management  
JPL*

*Mail Stop 202-233*

*4800 Oak Grove Drive*

*Pasadena, CA 91109-8099*

*(818) 354-2240*

*E-mail: iaoffice@jpl.nasa.gov*

*Refer to NPO-30912, volume and number of this NASA Tech Briefs issue, and the page number.*

## Prioritizing Scientific Data for Transmission

*NASA's Jet Propulsion Laboratory, Pasadena, California*

A software system has been developed for prioritizing newly acquired geological data onboard a planetary rover. The system has been designed to enable efficient use of limited communication resources by transmitting the data likely to have the most scientific value. This software operates onboard a rover by analyzing collected data, identifying potential scientific targets, and then using that information to prioritize data for transmission to Earth. Currently, the system is focused on the analysis of acquired images, although the general techniques are applicable to a wide range of data modalities. Image prioritization is performed using two main

steps. In the first step, the software detects features of interest from each image. In its current application, the system is focused on visual properties of rocks. Thus, rocks are located in each image and rock properties, such as shape, texture, and albedo, are extracted from the identified rocks. In the second step, the features extracted from a group of images are used to prioritize the images using three different methods: (1) identification of key target signature (finding specific rock features the scientist has identified as important), (2) novelty detection (finding rocks we haven't seen before), and (3) representative rock sampling (finding

the most average sample of each rock type). These methods use techniques such as K-means unsupervised clustering and a discrimination-based kernel classifier to rank images based on their interest level.

*This program was written by Rebecca Castano, Robert Anderson, Tara Estlin, Dennis DeCoste, Daniel Gaines, Dominic Mazzoni, Forest Fisher, and Michele Judd of Caltech for NASA's Jet Propulsion Laboratory. Further information is contained in a TSP (see page 1).*

*This software is available for commercial licensing. Please contact Don Hart of the California Institute of Technology at (818) 393-3425. Refer to NPO-40265.*

## Determining Sizes of Particles in a Flow From DPIV Data

**The same equipment would be used to measure sizes as well as velocities.**

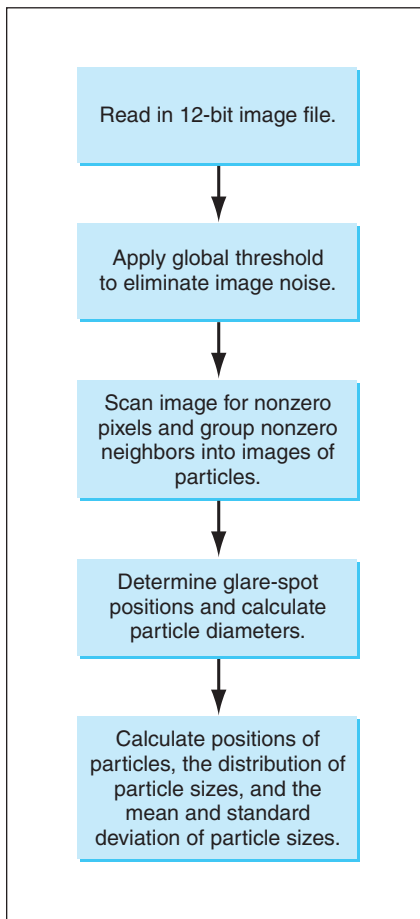
*John H. Glenn Research Center, Cleveland, Ohio*

A proposed method of measuring the size of particles entrained in a flow of a liquid or gas would involve utilization of data from digital particle-image velocimetry (DPIV) of the flow. That is to say, with proper design and operation of

a DPIV system, the DPIV data could be processed according to the proposed method to obtain particle sizes in addition to particle velocities. As an additional benefit, one could then compute the mass flux of the entrained particles

from the particle sizes and velocities.

As in DPIV as practiced heretofore, a pulsed laser beam would be formed into a thin sheet to illuminate a plane of interest in a flow field and the illuminated plane would be observed by means of a



The **Algorithm of the Proposed Method** would process DPIV data to extract information on particle sizes. The size information would be in addition to the velocity information extracted from the data by use of previously developed DPIV software.

charge-coupled device (CCD) camera aimed along a line perpendicular to the illuminated plane. Unlike in DPIV as practiced heretofore, care would be taken to polarize the laser beam so that its electric field would lie in the illuminated plane, for the reason explained in the next paragraph.

The proposed method applies, more specifically, to transparent or semitransparent spherical particles that have an index of refraction different from that of the fluid in which they are entrained. The method is based on the established Mie theory, which describes the scattering of light by diffraction, refraction, and specular reflection of light by such particles. In the case of a particle illuminated by polarized light and observed in the arrangement described in the preceding paragraph, the Mie theory shows that the image of the particle on the focal plane of the CCD camera includes two glare spots: one attributable to light reflected toward the camera and one attributable to light refracted toward the camera. The distance between the glare spots is a known function of the size of the particle, the indices of refraction of the particle material, and design parameters of the camera optics. Hence, the size of a particle can be determined from the distance between the glare spots.

The proposed method would be implemented in an algorithm that would automatically identify, and measure the distance between, the glare spots for each particle for which a suitable image has been captured in a DPIV image frame. The algorithm (see figure) would begin with thresholding of data from the entire image frame to reduce noise, thereby facilitating discrimination of particle images from the background and aiding in the separation of overlapping particles. It is important not to pick a threshold level so high that the light intensity between a given pair of glare spots does not fall below the threshold value, leaving the glare spots disconnected.

The image would then be scanned in a sequence of rows and columns of pixels to identify groups of adjacent pixels that contain nonzero brightnesses and that

are surrounded by pixels of zero brightness. Each such group would be assumed to constitute the image of one particle. Each such group would be further analyzed to determine whether the image was saturated; saturated particle images must be rejected because the locations of glare spots in saturated images cannot accurately be determined. Within each unsaturated particle image, the centroids (deemed to be the locations) of the glare spots would be determined by means of gradients of brightness distributions and three-point horizontal and three-point vertical Gaussian estimates based on the brightness values of the brightest pixels and the pixels adjacent to them. If the brightness of a given particle image contained only one peak, then it would be assumed that a second glare spot did not exist and that image would be rejected.

Once the centroids had been estimated for all particle images for which it was possible to do so, the positions of the particles and the distances between their centroids would be computed. As described above, the size of each particle would then be computed from the distance between its centroids. Finally, the distribution, mean, and standard deviation of sizes would be computed for the collection of particle images that survived to the final stage of the centroid-estimation process.

*This work was done by M. P. Wernet of Glenn Research Center and A. Mielke and J. R. Kadambi of Case Western Reserve University. Further information is contained in a TSP (see page 1).*

*Inquiries concerning rights for the commercial use of this invention should be addressed to NASA Glenn Research Center, Commercial Technology Office, Attn: Steve Fedor, Mail Stop 4-8, 21000 Brookpark Road, Cleveland, Ohio 44135. Refer to LEW-17340.*

## Faster Processing for Inverting GPS Occultation Data

NASA's Jet Propulsion Laboratory, Pasadena, California

A document outlines a computational method that can be incorporated into two prior methods used to invert Global Positioning System (GPS) occultation data [signal data acquired by a low-Earth-orbiting satellite as either this or the GPS satellite rises above or falls below the horizon] to obtain information on altitude-depen-

dent properties of the atmosphere. The two prior inversion methods, known as back propagation and canonical transform, are computationally expensive because for each occultation, they involve numerical evaluation of a large number of diffraction-like spatial integrals. The present method involves an angular-spectrum-based phase-ex-

trapolation approximation in which each data point is associated with a plane-wave component that propagates in a unique direction from the orbit of the receiving satellite to intersect a straight line tangent to the orbit at a nearby point. This approximation enables the use of fast Fourier transforms (FFTs), which apply only to data

collected along a straight-line trajectory. The computation of the diffraction-like integrals in the angular-spectrum domain by use of FFTs takes only seconds, whereas previously, it took minutes.

*This work was done by Chi Ao of Caltech for NASA's **Jet Propulsion Laboratory**. Further information is contained in a TSP (see page 1).*

*The software used in this innovation is available for commercial licensing. Please*

*contact Don Hart of the California Institute of Technology at (818) 393-3425. Refer to NPO-30791.*



## FPGA-Based, Self-Checking, Fault-Tolerant Computers

No software support and little hardware support would be needed for fault tolerance.

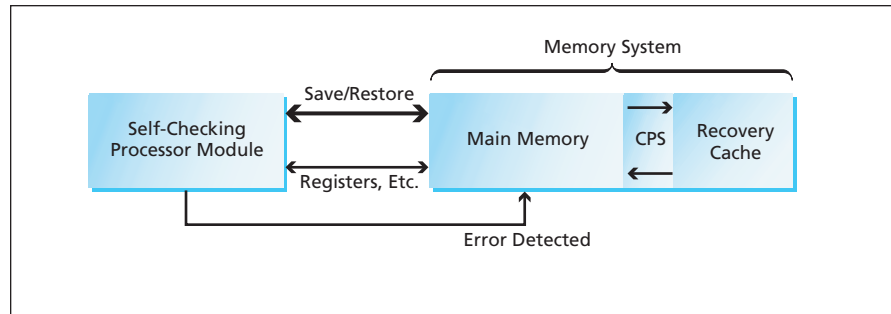
NASA's Jet Propulsion Laboratory, Pasadena, California

A proposed computer architecture would exploit the capabilities of commercially available field-programmable gate arrays (FPGAs) to enable computers to detect and recover from bit errors. The main purpose of the proposed architecture is to enable fault-tolerant computing in the presence of single-event upsets (SEUs). [An SEU is a spurious bit flip (also called a soft error) caused by a single impact of ionizing radiation.] The architecture would also enable recovery from some soft errors caused by electrical transients and, to some extent, from intermittent and permanent (hard) errors caused by aging of electronic components.

A typical FPGA of the current generation contains one or more complete processor cores, memories, and high-speed serial input/output (I/O) channels, making it possible to shrink a board-level processor node to a single integrated-circuit chip. Custom, highly efficient microcontrollers, general-purpose computers, custom I/O processors, and signal processors can be rapidly and efficiently implemented by use of FPGAs. Unfortunately, FPGAs are susceptible to SEUs. Prior efforts to mitigate the effects of SEUs have yielded solutions that degrade performance of the system and require support from external hardware and software.

In comparison with other fault-tolerant-computing architectures (e.g., triple modular redundancy), the proposed architecture could be implemented with less circuitry and lower power demand. Moreover, the fault-tolerant computing functions would require only minimal support from circuitry outside the central processing units (CPUs) of computers, would not require any software support, and would be largely transparent to software and to other computer hardware.

There would be two types of modules: a self-checking processor module and a memory system (see figure). The self-checking processor module would be implemented on a single FPGA and would be capable of detecting its own internal errors. It would contain two



The **Memory System** would store the states of computations at checkpoint intervals. Upon detection of an error in the self-checking processor module, the memory system would provide the information needed to roll back the computations to the immediately preceding checkpoint.

CPUs executing identical programs in lock step, with comparison of their outputs to detect errors. It would also contain various cache local memory circuits, communication circuits, and configurable special-purpose processors that would use self-checking checkers. (The basic principle of the self-checking checker method is to utilize logic circuitry that generates error signals whenever there is an error in either the checker or the circuit being checked.)

The memory system would comprise a main memory and a hardware-controlled check-pointing system (CPS) based on a buffer memory denoted the recovery cache. The main memory would contain random-access memory (RAM) chips and FPGAs that would, in addition to everything else, implement double-error-detecting and single-error-correcting memory functions to enable recovery from single-bit errors.

The main purpose served by the memory system as a whole would be to enable the computer to return to a valid state — a known good point reached in the computations before the occurrence of a detected error. In operation, the checkers in the self-checking processor module would signal errors to the memory system. Recovery would involve halting the operation of the self-checking processor module, correcting its configuration bits if necessary, reloading its registers, and returning control to a previous, known good point in the program. The CPUs could then resume correct computations.

The known good point in the computations would be provided by the CPS in a procedure denoted, variously, as checkpointing and checkpoint recovery or checkpoint rollback. The CPS would periodically command each CPU to store the contents of its registers in the recovery cache and clear its caches. This action would establish a checkpoint. Then the original value and the address of any clean RAM block that was subsequently overwritten by the CPU would be stored in a special RAM within the recovery cache. Subsequent writes to that block would be carried out normally (that is, without intervention by the recovery cache). If an error in the CPU were detected, the data in the special recovery-cache RAM could be used to restore the corresponding data in the main memory to their prior correct values, the processor configuration would be reloaded, the caches in the processor module would be cleared, and the processor registers restored to their prior values.

A new checkpoint could be ordered when the recovery cache became filled to capacity. Alternately, checkpoints could be forced at strategic points in the software. Another alternative would be to force checkpoints periodically, at intervals short enough to ensure that rollback time did not exceed a value that could be specified by design.

*This work was done by Raphael Some and David Rennels of Caltech for NASA's Jet Propulsion Laboratory. Further information is contained in a TSP (see page 1). NPO-30806*

# Ultralow-Power Digital Correlator for Microwave Polarimetry

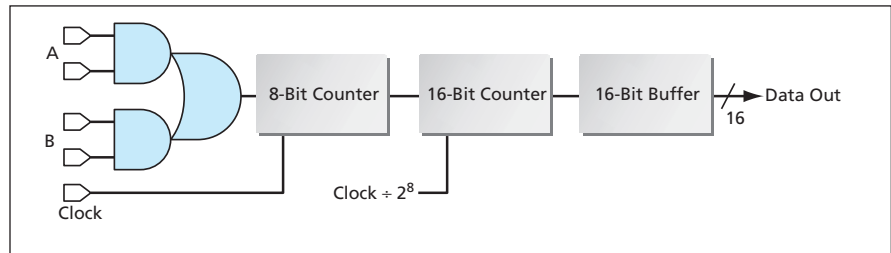
This circuit overcomes disadvantages of prior digital correlators.

Goddard Space Flight Center, Greenbelt, Maryland

A recently developed high-speed digital correlator is especially well suited for processing readings of a passive microwave polarimeter. This circuit computes the auto-correlations of, and the cross-correlations among, data in four digital input streams representing samples of in-phase (I) and quadrature (Q) components of two intermediate-frequency (IF) signals, denoted A and B, that are generated in heterodyne reception of two microwave signals.

The IF signals arriving at the correlator input terminals have been digitized to three levels (-1,0,1) at a sampling rate up to 500 MHz. Two bits (representing sign and magnitude) are needed to represent the instantaneous datum in each input channel; hence, eight bits are needed to represent the four input signals during any given cycle of the sampling clock. The accumulation (integration) time for the correlation is programmable in increments of  $2^8$  cycles of the sampling clock, up to a maximum of  $2^{24}$  cycles.

The basic functionality of the correlator is embodied in 16 correlation slices, each of which contains identical logic circuits and counters (see figure). The first stage of each correlation slice is a logic gate that computes one of the desired correlations (for example, the autocorrelation of the I component of A or the negative of the cross-correlation of the I component of A and the Q component of B). The sampling of the output of the logic gate output is controlled by the sampling-clock signal, and an 8-bit counter increments in every clock cycle when the



A **Correlation Slice** is one of 16 identical units that embody the basic functionality of the high-speed, ultralow-power digital correlator.

logic gate generates output. The most significant bit of the 8-bit counter is sampled by a 16-bit counter with a clock signal at  $2^8$  the frequency of the sampling clock. The 16-bit counter is incremented every time the 8-bit counter rolls over.

The correlator is designed for use with a microprocessor. The microprocessor controls the function of the correlator, sets the desired integration time by writing appropriate values to registers in the correlator, and reads the correlation outputs as described next. At the end of the integration period, the contents of the 16-bit counter are copied to a 16-bit buffer, and the 16-bit counter is cleared to begin a new accumulation cycle. At the same time, the correlator generates a signal to indicate, to the microprocessor, that new correlation data are available. The correlator and the microprocessor communicate via a simple 3.3-V bus-oriented interface, such that from the perspective of the microprocessor, the correlator acts much like a small random-access memory containing 32

16-bit words. Hence, the microprocessor reads the correlation-slice buffers by supplying five-bit addresses to select the buffers as a group of memory locations.

The correlator has been implemented as a complementary metal oxide/semiconductor (CMOS) integrated circuit, following 0.35- $\mu\text{m}$  radiation tolerant design rules. The main advantage of this high-speed digital correlator over prior ones is ultralow-power dissipation: whereas a previous high-speed digital correlator dissipates a power of about 10 W (and processes only two input data streams), this correlator dissipates a power of 2 mW or less, the exact value depending on the sampling rate. To achieve such ultralow-power operation a logic level of only 0.5 V is used, necessitating the use of special signal-conditioning circuits.

*This work was done by Jeffrey R. Piepmeier of Goddard Space Flight Center and K. Joseph Hass of the University of Idaho. Further information is contained in a TSP (see page 1). GSC-14746-1*

# Grounding Headphones for Protection Against ESD

John F. Kennedy Space Center, Florida

A simple alternative technique has been devised protecting delicate equipment against electrostatic discharge (ESD) in settings in which workers wear communication headsets. In the original setting in which the technique was devised, the workers who wear the headsets also wear anti-ESD grounding straps on their wrists. The alternative technique eliminates the need for the wrist grounding straps by providing for grounding through the headsets. In place of the electrically insulating foam pads on the

headsets, one installs pads made of electrically conductive foam like that commonly used to protect electronic components. Grounding wires are attached to the conductive foam pads, then possibly to the shielding cable which may be grounded to the backshell on the connector. The efficacy of this technique in protecting against ESD has been verified in experiments. The electrical resistance of the pads is a few megohms — about the same as that of a human body between the fingers of opposite hands and,

hence, low enough for grounding. The only drawback of the technique is that care must be taken to place the foam pads in contact with the user's skin: any hair that comes between the foam pads and the skin must be pushed aside because hair is electrically insulating and thus prevents adequate grounding.

*This work was done by John Peters and Robert C. Youngquist of Kennedy Space Center. For further information, contact the Kennedy Commercial Technology Office at 321-867-1463. KSC-12295*

# Lightweight Stacks of Direct Methanol Fuel Cells

Power-to-mass ratios can be tripled.

NASA's Jet Propulsion Laboratory, Pasadena, California

An improved design concept for direct methanol fuel cells makes it possible to construct fuel-cell stacks that can weigh as little as one-third as much as do conventional bipolar fuel-cell stacks of equal power. The structural-support components of the improved cells and stacks can be made of relatively inexpensive plastics. Moreover, in comparison with conventional bipolar fuel-cell stacks, the improved fuel-cell stacks can be assembled, disassembled, and diagnosed for malfunctions more easily. These improvements are expected to bring portable direct methanol fuel cells and stacks closer to commercialization.

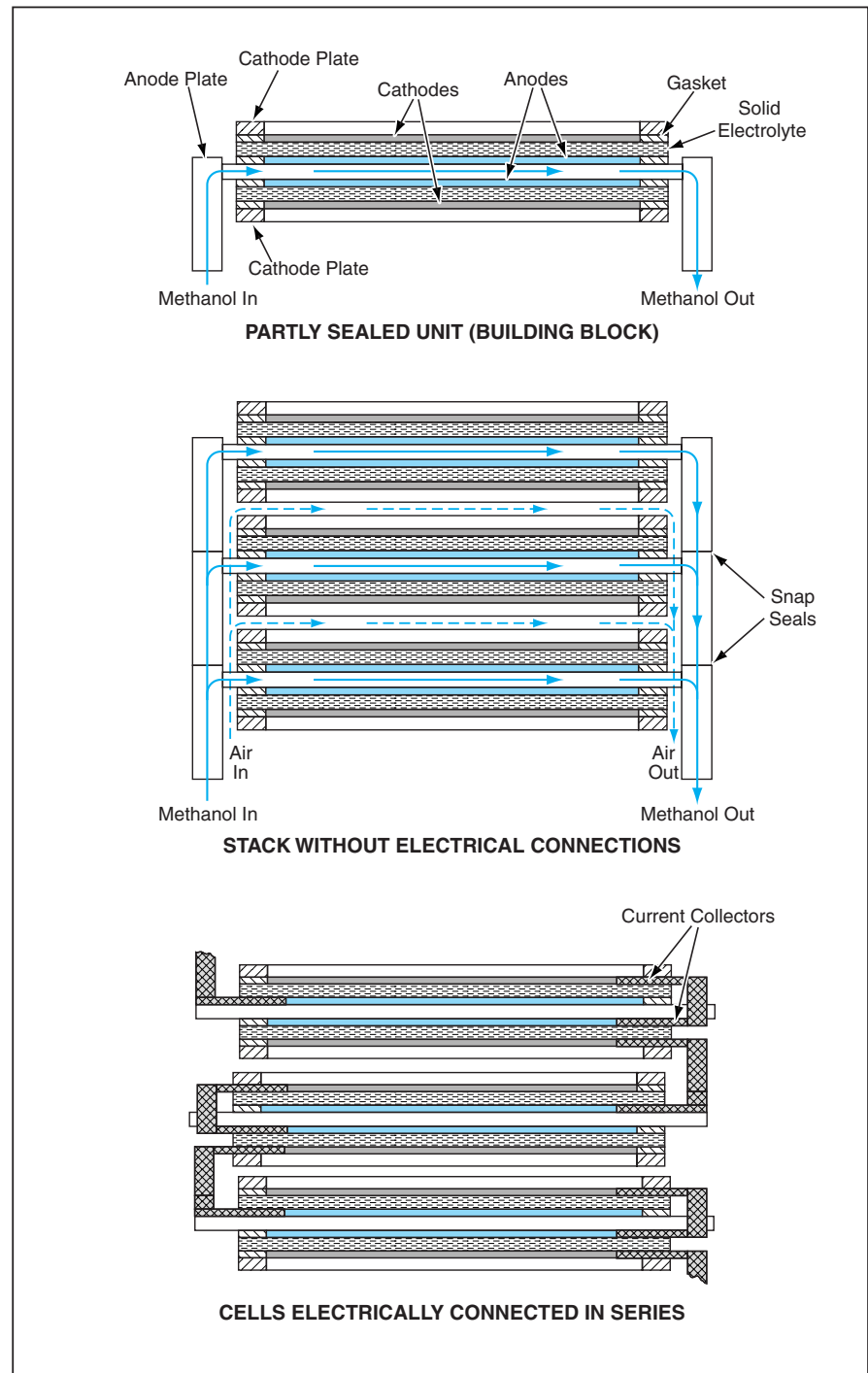
In a conventional bipolar fuel-cell stack, the cells are interspersed with bipolar plates (also called biplates), which are structural components that serve to interconnect the cells and distribute the reactants (methanol and air). The cells and biplates are sandwiched between metal end plates. Usually, the stack is held together under pressure by tie rods that clamp the end plates. The bipolar stack configuration offers the advantage of very low internal electrical resistance. However, when the power output of a stack is only a few watts, the very low internal resistance of a bipolar stack is not absolutely necessary for keeping the internal power loss acceptably low.

Typically, about 80 percent of the mass of a conventional bipolar fuel-cell stack resides in the biplates, end plates, and tie rods. The biplates are usually made of graphite composites and must be molded or machined to contain flow channels, at a cost that is usually a major part of the total cost of the stack. In the event of a malfunction in one cell, it is necessary to disassemble the entire stack in order to be able to diagnose that cell. What is needed is a design that reduces the mass of the stack, does not require high pressure to ensure sealing, is more amenable to troubleshooting, and reduces the cost of manufacture.

The present improved design satisfies these needs and is especially suitable for applications in which the power demand is  $\leq 20$  W. This design eliminates the biplates, end plates, and tie rods. In this design, the basic build-

ing block of a stack is a sealed unit that contains an anode plate, two cathode plates, and two back-to-back cells (see figure). The structural-support and flow-channeling components of the

units are made from inexpensive plastics. Each unit is assembled and tested separately, then the units are assembled into the stack. The units are joined by simple snap seals similar to



Partly Sealed Units Are Joined by Snap Seals and their current collectors are connected together to form a fuel-cell stack. Each sealed unit contains a back-to-back pair of fuel cells.

the zipperlike seals on plastic bags commonly used to store food. The cathode and anode plates include current collectors, the inside ends of which are electrically connected to the electrodes and the outer ends of which can be used to form the desired series and/or parallel electrical connections among the cells. Because the stack need not be clamped or otherwise held together under pressure, the stack can

easily be disassembled to replace a malfunctioning sealed unit.

*This work was done by Sekharipuram Narayanan and Thomas Valdez of Caltech for NASA's Jet Propulsion Laboratory. Further information is contained in a TSP (see page 1).*

*In accordance with Public Law 96-517, the contractor has elected to retain title to this invention. Inquiries concerning rights for its commercial use should be*

*addressed to*

*Intellectual Assets Office*

*JPL*

*Mail Stop 202-233*

*4800 Oak Grove Drive*

*Pasadena, CA 91109*

*(818) 354-2240*

*E-mail: ipgroup@jpl.nasa.gov*

*Refer to NPO-30570, volume and number of this NASA Tech Briefs issue, and the page number.*

---

## Highly Efficient Vector-Inversion Pulse Generators

*Marshall Space Flight Center, Alabama*

Improved transmission-line pulse generators of the vector-inversion type are being developed as lightweight sources of pulsed high voltage for diverse applications, including spacecraft thrusters, portable x-ray imaging systems, impulse radar systems, and corona-discharge systems for sterilizing gases. In this development, more than the customary attention is paid to principles of operation and details of construction so as to maximize the efficiency of the pulse-generation

process while minimizing the sizes of components. An important element of this approach is segmenting a pulse generator in such a manner that the electric field in each segment is always below the threshold for electrical breakdown. One design of particular interest, a complete description of which was not available at the time of writing this article, involves two parallel-plate transmission lines that are wound on a mandrel, share a common conductor, and are switched in such

a manner that the pulse generator is divided into a "fast" and a "slow" section. A major innovation in this design is the addition of ferrite to the "slow" section to reduce the size of the mandrel needed for a given efficiency.

*This work was done by M. Franklin Rose of Radianc Technologies, Inc., for Marshall Space Flight Center. Further information is contained in a TSP (see page 1).*  
*MFS-31870*

## Estimating Basic Preliminary Design Performances of Aerospace Vehicles

Aerodynamics and Performance Estimation Toolset is a collection of four software programs for rapidly estimating the preliminary design performance of aerospace vehicles represented by doing simplified calculations based on ballistic trajectories, the ideal rocket equation, and supersonic wedges through standard atmosphere. The program consists of a set of Microsoft Excel worksheet subprograms. The input and output data are presented in a user-friendly format, and calculations are performed rapidly enough that the user can iterate among different trajectories and/or shapes to perform “what-if” studies. Estimates that can be computed by these programs include:

1. Ballistic trajectories as a function of departure angles, initial velocities, initial positions, and target altitudes; assuming point masses and no atmosphere. The program plots the trajectory in two-dimensions and outputs the position, pitch, and velocity along the trajectory.
2. The “Rocket Equation” program calculates and plots the trade space for a vehicle’s propellant mass fraction over a range of specific impulse and mission velocity values, propellant mass fractions as functions of specific impulses and velocities.
3. “Standard Atmosphere” will estimate the temperature, speed of sound, pressure, and air density as a function of altitude in a standard atmosphere, properties of a standard atmosphere as functions of altitude.
4. “Supersonic Wedges” will calculate the free-stream, normal-shock, oblique-shock, and isentropic flow properties for a wedge-shaped body flying supersonically through a standard atmosphere. It will also calculate the maximum angle for which a shock remains attached, and the minimum Mach number for which a shock becomes attached, all as functions of the wedge angle, altitude, and Mach number.

*This work was done by Paul L. Luz and Reginald Alexander of Marshall Space Flight Center. For further information, contact Caroline Wang, MSFC Software Release Authority, at (256) 544-3887 or Caroline.K.Wang@nasa.gov. Refer to MFS-31795.*

## Framework for Development of Object-Oriented Software

The Real-Time Control (RTC) Application Framework is a high-level software framework written in C++ that supports the rapid design and implementation of object-oriented application programs. This framework provides built-in functionality that solves common software development problems within distributed client-server, multi-threaded, and embedded programming environments. When using the RTC Framework to develop software for a specific domain, designers and implementers can focus entirely on the details of the domain-specific software rather than on creating custom solutions, utilities, and frameworks for the complexities of the programming environment. The RTC Framework was originally developed as part of a Space Shuttle Launch Processing System (LPS) replacement project called Checkout and Launch Control System (CLCS). As a result of the framework’s development, CLCS software development time was reduced by 66 percent. The framework is generic enough for developing applications outside of the launch-processing system domain. Other applicable high-level domains include command and control systems and simulation/training systems.

*This software was written by Gus Perez-Poveda of 360 Software Corporation, Tony Ciavarella of United Space Alliance, and Dan Nieten of Kennedy Space Center. For further information, access <http://www.360SoftwareCorp.com>.*

*In accordance with Public Law 96-517, the contractor has elected to retain title to this invention. Inquiries concerning rights for its commercial use should be addressed to:*

*360 Software Corporation  
12472 Lake Underhill Rd. #174  
Orlando, FL 32828  
Phone: (407) 694-2227*

*Refer to KSC-12499, volume and number of this NASA Tech Briefs issue, and the page number.*

## Analyzing Spacecraft Telecommunication Systems

Multi-Mission Telecom Analysis Tool (MMTAT) is a C-language computer program for analyzing proposed spacecraft telecommunication systems. MMTAT uti-

lizes parameterized input and computational models that can be run on standard desktop computers to perform fast and accurate analyses of telecommunication links. MMTAT is easy to use and can easily be integrated with other software applications and run as part of almost any computational simulation. It is distributed as either a stand-alone application program with a graphical user interface or a linkable library with a well-defined set of application programming interface (API) calls. As a stand-alone program, MMTAT provides both textual and graphical output. The graphs make it possible to understand, quickly and easily, how telecommunication performance varies with variations in input parameters. A delimited text file that can be read by any spreadsheet program is generated at the end of each run. The API in the linkable-library form of MMTAT enables the user to control simulation software and to change parameters during a simulation run. Results can be retrieved either at the end of a run or by use of a function call at any time step.

*This program was written by Mark Kordon, David Hanks, Roy Gladden, and Eric Wood of Caltech for NASA’s Jet Propulsion Laboratory. Further information is contained in a TSP (see page 1).*

*This software is available for commercial licensing. Please contact Don Hart of the California Institute of Technology at (818) 393-3425. Refer to NPO-40298.*

## Collaborative Planning of Robotic Exploration

The Science Activity Planner (SAP) software system includes an uplink-planning component, which enables collaborative planning of activities to be undertaken by an exploratory robot on a remote planet or on Earth. Included in the uplink-planning component is the SAP-Uplink Browser, which enables users to load multiple spacecraft activity plans into a single window, compare them, and merge them. The uplink-planning component includes a subcomponent that implements the Rover Markup Language Activity Planning format (RML-AP), based on the Extensible Markup Language (XML) format that enables the representation, within a single document, of planned spacecraft and robotic activities together with the scientific rea-

sons for the activities. Each such document is highly parseable and can be validated easily. Another subcomponent of the uplink-planning component is the Activity Dictionary Markup Language (ADML), which eliminates the need for two mission activity dictionaries — one in a human-readable format and one in a machine-readable format. Style sheets that have been developed along with the ADML format enable users to edit one dictionary in a user-friendly environment without compromising the machine-readability of the format.

*This program was written by Jeffrey Norris, Paul Backes, Mark Powell, Marsette Vona, and Robert Steinke of Caltech for NASA's Jet Propulsion Laboratory. Further information is contained in a TSP (see page 1).*

*This software is available for commercial licensing. Please contact Don Hart of the California Institute of Technology at (818) 393-3425. Refer to NPO-30676.*

## Tools for Administration of a UNIX-Based Network

Several computer programs have been developed to enable efficient administration of a large, heterogeneous, UNIX-based computing and communication network that includes a variety of computers connected to a variety of sub-networks. One program provides secure software tools for administrators to create, modify, lock, and delete accounts of specific users. This program also provides tools for users to change their UNIX passwords and log-in shells. These tools check for errors. Another program comprises a client and a server component that, together, provide a secure mechanism to create, modify, and query quota levels on a network file system (NFS) mounted by use of the VERITAS File SystemJ software. The client software resides on an internal secure computer with a secure Web interface; one can gain access to the client software from any authorized computer capable of running web-browser software. The

server software resides on a UNIX computer configured with the VERITAS software system. Directories where VERITAS quotas are applied are NFS-mounted. Another program is a Web-based, client/server Internet Protocol (IP) address tool that facilitates maintenance lookup of information about IP addresses for a network of computers.

*These programs were written by Stephen LeClaire and Edward Farrar of Netlander, Inc., for Kennedy Space Center. For further information, contact the Kennedy Commercial Technology Office at (321) 867-1463. KSC-12269/68/71*

## Preparing and Analyzing Iced Airfoils

SmaggIce version 1.2 is a computer program for preparing and analyzing iced airfoils. It includes interactive tools for (1) measuring ice-shape characteristics, (2) controlled smoothing of ice shapes, (3) curve discretization, (4) generation of artificial ice shapes, and (5) detection and correction of input errors. Measurements of ice shapes are essential for establishing relationships between characteristics of ice and effects of ice on airfoil performance. The shape-smoothing tool helps prepare ice shapes for use with already available grid-generation and computational-fluid-dynamics software for studying the aerodynamic effects of smoothed ice on airfoils. The artificial ice-shape generation tool supports parametric studies since ice-shape parameters can easily be controlled with the artificial ice. In such studies, artificial shapes generated by this program can supplement simulated ice obtained from icing research tunnels and real ice obtained from flight test under icing weather condition. SmaggIce also automatically detects geometry errors such as tangles or duplicate points in the boundary which may be introduced by digitization and provides tools to correct these. By use of interactive tools included in SmaggIce version 1.2, one can easily characterize ice shapes

and prepare iced airfoils for grid generation and flow simulations.

*This program was written by Mary B. Vickerman, Marivell Baez, Donald C. Braun, Barbara J. Cotton, Yung K. Choo, Rula M. Coroneos, James A. Pennline, Anthony W. Hackenberg, and Herbert W. Schilling of Glenn Research Center. John W. Slater with Yung K. Choo contributed to the conception of the code. In addition, Kevin M. Burke, Gerald J. Nolan, and Dennis Brown of InDyne, Inc., contributed to developing training material. For further information, access <http://icebox-esn.grc.nasa.gov/ext/design/smaggice.html>.*

*Inquiries concerning rights for the commercial use of this invention should be addressed to NASA Glenn Research Center, Commercial Technology Office, Attn: Steve Fedor, Mail Stop 4-8, 21000 Brookpark Road, Cleveland, Ohio 44135. Refer to LEW-17399.*

## Evaluating Performance of Components

Parallel Component Performance Benchmarks is a computer program developed to aid the evaluation of the Common Component Architecture (CCA) — a software architecture, based on a component model, that was conceived to foster high-performance computing, including parallel computing. More specifically, this program compares the performances (principally by measuring computing times) of componentized versus conventional versions of the Parallel Pyramid 2D Adaptive Mesh Refinement library — a software library that is used to generate computational meshes for solving physical problems and that is typical of software libraries in use at NASA's Jet Propulsion Laboratory.

*This program was written by Daniel Katz, Edwin Tisdale, and Charles Norton of Caltech for NASA's Jet Propulsion Laboratory. Further information is contained in a TSP (see page 1).*

*This software is available for commercial licensing. Please contact Don Hart of the California Institute of Technology at (818) 393-3425. Refer to NPO-30693.*



## **Fuels Containing Methane or Natural Gas in Solution**

**A blend of gasoline and natural gas offers advantages over alternative fuels.**

*Lyndon B. Johnson Space Center, Houston, Texas*

While exploring ways of producing better fuels for propulsion of a spacecraft on the Mars sample return mission, a researcher at Johnson Space Center (JSC) devised a way of blending fuel by combining methane or natural gas with a second fuel to produce a fuel that can be maintained in liquid form at ambient temperature and under moderate pressure. The use of such a blended fuel would be a departure for both spacecraft engines and terrestrial internal combustion engines. For spacecraft, it would enable reduction of weights on long flights. For the automotive industry on Earth, such a fuel could be easily distributed and could be a less expensive, more efficient, and cleaner-burning alternative to conventional fossil fuels.

The concept of blending fuels is not new: for example, the production of gasoline includes the addition of liquid octane enhancers. For the future, it has been commonly suggested to substitute methane or compressed natural gas for octane-enhanced gasoline as a fuel for internal-combustion engines. Unfortunately, methane or natural gas must be stored either as a compressed gas (if kept at ambient temperature) or as a cryogenic liquid. The ranges of automobiles would be reduced from their present val-

ues because of limitations on the capacities for storage of these fuels. Moreover, technical challenges are posed by the need to develop equipment to handle these fuels and, especially, to fill tanks acceptably rapidly. The JSC alternative — to provide a blended fuel that can be maintained in liquid form at moderate pressure at ambient temperature — has not been previously tried.

A blended automotive fuel according to this approach would be made by dissolving natural gas in gasoline. The auto-genous pressure of this fuel would eliminate the need for a vehicle fuel pump, but a pressure and/or flow regulator would be needed to moderate the effects of temperature and to respond to changing engine power demands. Because the fuel would flash as it entered engine cylinders, relative to gasoline, it would disperse more readily and therefore would mix with air more nearly completely. As a consequence, this fuel would burn more nearly completely (and, hence, more cleanly) than gasoline does.

The storage density of this fuel would be similar to that of gasoline, but its energy density would be such that the mileage (more precisely, the distance traveled per unit volume of fuel) would be greater than that of either gasoline or

compressed natural gas. Because the pressure needed to maintain the fuel in liquid form would be more nearly constant and generally lower than that needed to maintain compressed natural gas in liquid form, the pressure rating of a tank used to hold this fuel could be lower than that of a tank used to hold compressed natural gas.

A mixture of natural gas and gasoline could be distributed more easily than could some alternative fuels. A massive investment in new equipment would not be necessary: One could utilize the present fuel-distribution infrastructure and could blend the gasoline and natural gas at almost any place in the production or distribution process — perhaps even at the retail fuel pump. Yet another advantage afforded by use of a blend of gasoline and natural gas would be a reduction in the amount of gasoline consumed. Because natural gas costs less than gasoline does and is in abundant supply in the United States, the cost of automotive fuel and the demand for imported oil could be reduced.

*This work was done by Thomas A. Sullivan of Johnson Space Center. For further information, contact the Johnson Commercial Technology Office at (281) 483-3809. Refer to MSC-22873.*

## **Direct Electrolytic Deposition of Mats of $Mn_xO_y$ Nanowires**

**These mats of nanowires can be used as electrodes for batteries and capacitors.**

*NASA's Jet Propulsion Laboratory, Pasadena, California*

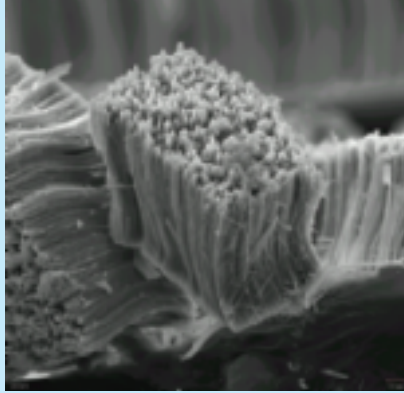
Mats of free-standing manganese oxide ( $Mn_xO_y$ ) nanowires have been fabricated as experimental electrode materials for rechargeable electrochemical power cells and capacitors. Because they are free-standing, the wires in these mats are electrochemically accessible. The advantage of the mat-of-nanowires configuration, relative to other configurations of electrode materials, arises from the combination of narrowness and high areal number density of the wires. This combination offers both high

surface areas for contact with electrolytes and short paths for diffusion of ions into and out of the electrodes, thereby making it possible to charge and discharge at rates higher than would otherwise be possible and, consequently, to achieve greater power densities.

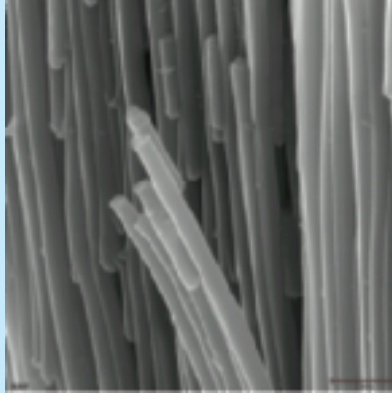
The nanowires are fabricated in an electrolytic process in which there is no need for an electrode binder material. Moreover, there is no need to incorporate an electrically conductive additive into the electrode material; the only

electrically conductive material that must be added is a thin substrate contact film at the anchored ends of the nanowires. Hence, the mass fraction of active electrode material is close to 100 percent, as compared with about 85 percent in conventional electrodes made from a slurry of active electrode material, binder, and conductive additive pressed onto a metal foil.

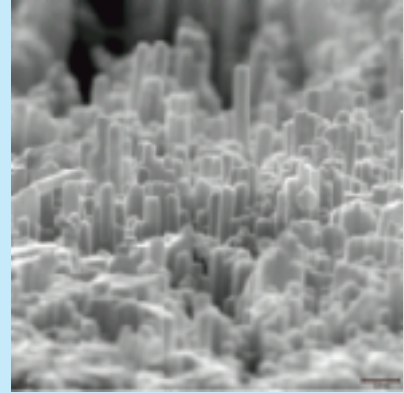
The locations and sizes of the nanowires are defined by holes in templates in the form of commercially avail-



Cross-Sectional View (Low Magnification)



Cross-Sectional View (High Magnification)



Top View

These **Free-Standing Mn<sub>x</sub>O<sub>y</sub> Wires** were made by electrodeposition of Mn<sub>x</sub>O<sub>y</sub> in 20-nm-wide pores in an alumina membrane, then dissolving the membrane in a concentrated alkaline solution.

able porous alumina membranes. In experiments to demonstrate the present process, alumina membranes of various pore sizes and degrees of porosity were used. First, a film of Au was sputtered onto one side of each membrane. The membranes were then attached, variously, to carbon tape or a gold substrate by use of silver or carbon paste. Once thus attached, the membranes were immersed in a plating solution comprising 0.01 M MnSO<sub>4</sub> + 0.03 M (NH<sub>4</sub>)<sub>2</sub>SO<sub>4</sub>. The pH of the solution was kept constant at 8 by addition of H<sub>2</sub>SO<sub>4</sub> or NH<sub>4</sub>OH as needed. Mn<sub>x</sub>O<sub>y</sub> nanowires were poten-

tially electrodeposited in the pores in the alumina templates. Depending on the anodic deposition potentials, Mn<sub>x</sub>O<sub>y</sub> was deposited in various oxidation states [divalent (Mn<sub>3</sub>O<sub>4</sub>), trivalent (Mn<sub>2</sub>O<sub>3</sub>), or tetravalent (MnO<sub>2</sub>)]. The Mn<sub>x</sub>O<sub>y</sub> wires were made free-standing (see figure) by dissolving the alumina templates, variously, in KOH or NaOH at a concentration of 20 volume percent.

*This work was done by Nosang Myung, William West, Jay Whitacre, and Ratnakumar Bugga of Caltech for NASA's Jet Propulsion Laboratory. Further information is contained in a TSP (see page 1).*

*In accordance with Public Law 96-517, the contractor has elected to retain title to this invention. Inquiries concerning rights for its commercial use should be addressed to:*

*Innovative Technology Assets Management  
JPL*

*Mail Stop 202-233  
4800 Oak Grove Drive  
Pasadena, CA 91109-8099  
(818) 354-2240*

*E-mail: iaoffice@jpl.nasa.gov*

*Refer to NPO-30655, volume and number of this NASA Tech Briefs issue, and the page number.*



## ⊕ Bubble Eliminator Based on Centrifugal Flow

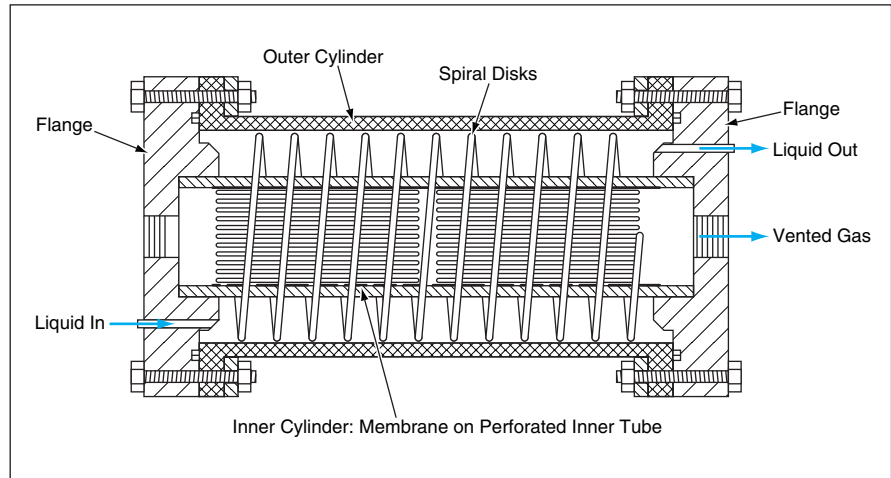
**This device contains no moving parts.**

*Lyndon B. Johnson Space Center, Houston, Texas*

The fluid bubble eliminator (FBE) is a device that removes gas bubbles from a flowing liquid. The FBE contains no moving parts and does not require any power input beyond that needed to pump the liquid. In the FBE, the buoyant force for separating the gas from the liquid is provided by a radial pressure gradient associated with a centrifugal flow of the liquid and any entrained bubbles. A device based on a similar principle is described in "Centrifugal Adsorption Cartridge System" (MSC-22863), which appears on page 48 of this issue. The FBE was originally intended for use in filtering bubbles out of a liquid flowing relatively slowly in a bioreactor system in microgravity. Versions that operate in normal Earth gravitation at greater flow speeds may also be feasible.

The FBE (see figure) is constructed as a cartridge that includes two concentric cylinders with flanges at the ends. The outer cylinder is an impermeable housing; the inner cylinder comprises a gas-permeable, liquid-impermeable membrane covering a perforated inner tube. Multiple spiral disks that collectively constitute a spiral ramp are mounted in the space between the inner and outer cylinders.

The liquid enters the FBE through an end flange, flows in the annular space between the cylinders, and leaves through the opposite end flange. The spiral disks channel the liquid into a spiral flow, the circumferential component of which gives rise to the desired centrifugal effect. The resulting radial pressure gradient forces the bubbles radially inward; that is,



The **Spiral Disks Channel the Liquid** into a spiral flow, which gives rise to a pressure gradient that drives bubbles toward the inner cylinder.

toward the inner cylinder. At the inner cylinder, the gas-permeable, liquid-impermeable membrane allows the bubbles to enter the perforated inner tube while keeping the liquid in the space between the inner and outer cylinders. The gas thus collected can be vented via an end-flange connection to the inner tube.

The centripetal acceleration (and thus the radial pressure gradient) is approximately proportional to the square of the flow speed and approximately inversely proportional to an effective radius of the annular space. For a given FBE geometry, one could increase the maximum rate at which gas could be removed by increasing the rate of flow to obtain more centripetal acceleration. In experiments and calculations oriented toward the original micro-

gravitational application, centripetal accelerations between 0.001 and 0.012  $g$  [where  $g \equiv$  normal Earth gravitation ( $\approx 9.8 \text{ m/s}^2$ )] were considered. For operation in normal Earth gravitation, it would likely be necessary to choose the FBE geometry and the rate of flow to obtain centripetal acceleration comparable to or greater than  $g$ .

*This work was done by Steve R. Gonda of Johnson Space Center and Yow-Min D. Tsao and Wenshan Lee of Wyle Laboratories. For further information, contact the Johnson Commercial Technology Office at 281-483-3809.*

*This invention is owned by NASA, and a patent application has been filed. Inquiries concerning nonexclusive or exclusive license for its commercial development should be addressed to the Patent Counsel, Johnson Space Center, (281) 483-0837. Refer to MSC-22996.*

## ⊕ Inflatable Emergency Atmospheric-Entry Vehicles

**Ballutes would act as inexpensive, lightweight atmospheric decelerator "lifeboats."**

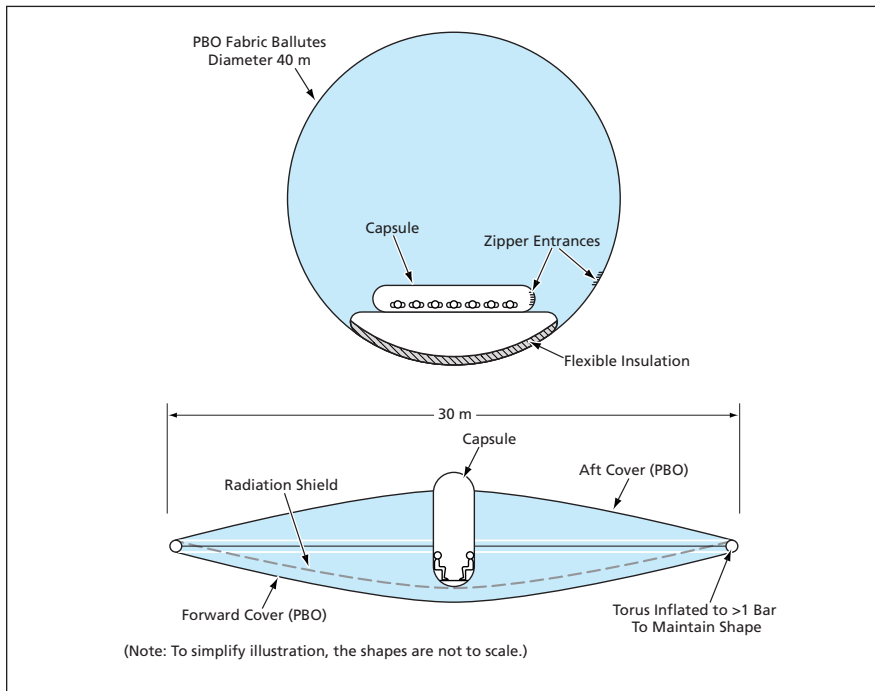
*NASA's Jet Propulsion Laboratory, Pasadena, California*

In response to the loss of seven astronauts in the Space Shuttle Columbia disaster, large, lightweight, inflatable atmospheric-entry vehicles have been proposed as means of emergency descent and landing for persons who must abandon a

spacecraft that is about to reenter the atmosphere and has been determined to be unable to land safely. Such a vehicle would act as an atmospheric decelerator at supersonic speed in the upper atmosphere, and a smaller, central astronaut

pod could then separate at lower altitudes and parachute separately to Earth.

Astronaut-rescue systems that have been considered previously have been massive, and the cost of designing them has exceeded the cost of fabrication of a



A Spherical Ballute (upper) and a Lens-Shaped Ballute (lower) have been considered for inflatable emergency atmospheric-entry vehicles.

space shuttle. In contrast, an inflatable emergency-landing vehicle according to the proposal would have a mass between 100 and 200 kg, could be stored in a volume of approximately 0.2 to 0.4 m<sup>3</sup>, and could likely be designed and built much less expensively.

When fully inflated, the escape vehicle behaves as a large balloon parachute, or ballute. Due to very low mass-per-surface area, a large radius, and a large coefficient of drag, ballutes decelerate at much higher altitudes and with

much lower heating rates than the space shuttle. Although the space shuttle atmospheric reentry results in surface temperatures of about 1,600 °C, ballutes can be designed for maximum temperatures below 600 °C. This allows ballutes to be fabricated with lightweight ZYLON<sup>®</sup>, or polybenzoxazole (PBO), or equivalent.

Two preliminary cocoon ballute “lifeboat” concepts are shown in the figures. The cocoon portion of the vehicle would be, more specifically, a capsule

pressurized to 1 bar (0.1 MPa — approximately 1 standard atmosphere). Crewmembers would enter the cocoon pod and then zip it shut. The spacecraft would be placed on a reentry trajectory, and the inflated cocoon with deflated ballute would be ejected.

Once the vehicle was safely away from the spacecraft, the entire ballute would be inflated. For this inflation at high altitude, the ballute would be pressurized to about 0.01 bar (1 kPa). As low as this pressure is, it is at least ten times the expected dynamic pressure on the vehicle during the heating portion of very high atmospheric reentry, and hence it is sufficient to enable the ballute to retain its shape. From thermal reentry heating analyses performed at JPL, the diameter of the inflated ballute would be made large enough (30 to 40 m) to limit the maximum temperature to about 500 °C — safely below the 600 °C limit for PBO, or equivalent.

The spherical ballute shown in the upper figure would have a mass of about 200 kg for a seven-astronaut rescue mission, while the lens-shaped ballute in the lower figure has been further improved by reducing the overall mass required and increasing the coefficient of drag. To maintain stability, the center of mass of both concepts must be kept low, and spin stabilization may be necessary.

*This work was done by Jack Jones, Jeffrey Hall, and Jiunn Jeng Wu of Caltech for NASA's Jet Propulsion Laboratory. Further information is contained in a TSP (see page 1).*

NPO-40156

## ⊕ Lightweight Deployable Mirrors With Tensegrity Supports

Extremely lightweight, deployable structures could be made by assembling tensegrity modules.

Marshall Space Flight Center, Alabama

The upper part of Figure 1 shows a small-scale prototype of a developmental class of lightweight, deployable structures that would support panels in precise alignments. In this case, the panel is hexagonal and supports disks that represent segments of a primary mirror of a large telescope. The lower part of Figure 1 shows a complete conceptual structure containing multiple hexagonal panels that hold mirror segments.

The structures of this class are of the tensegrity type, which was invented five decades ago by artist Kenneth Snelson. A

tensegrity structure consists of moment-free compression members (struts) and tension members (cables). The structures of this particular developmental class are intended primarily as means to erect large segmented primary mirrors of astronomical telescopes or large radio antennas in outer space. Other classes of tensegrity structures could also be designed for terrestrial use as towers, masts, and supports for general structural panels.

An important product of the present development effort is the engineering practice of building a lightweight, de-

ployable structure as an assembly of tensegrity modules like the one shown in Figure 2. This module comprises two octahedral tensegrity subunits that are mirror images of each other joined at their plane of mirror symmetry. In this case, the plane of mirror symmetry is both the upper plane of the lower subunit and the lower plane of the upper subunit, and is delineated by the mid-height triangle in Figure 2. In the configuration assumed by the module to balance static forces under mild loading, the upper and lower planes of each sub-

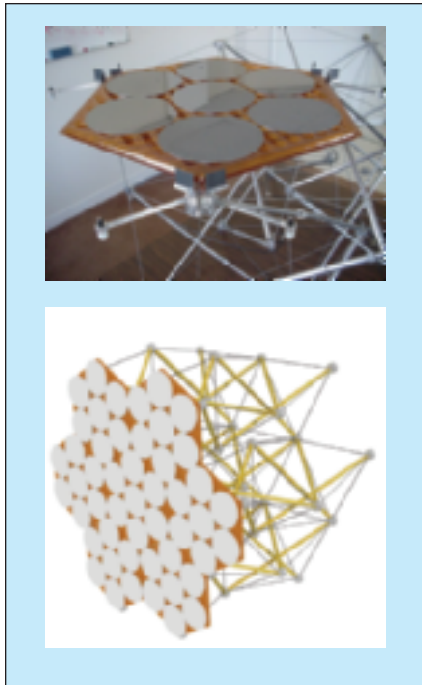


Figure 1. A **Tensegrity Structure** supports a lightweight, thermally formed, hexagonal plastic panel that, in turn, supports silicon disks that represent segments of an astronomical mirror. A fully developed version would comprise a hexagonal array of multiple hexagonal panels on a supporting tensegrity structure.

unit are rotated about 30°, relative to each other, about the long (vertical) axis of the structure. Larger structures can be assembled by joining multiple modules like this one at their sides or ends.

When the module is compressed axially (vertically), the first-order effect is



Figure 2. This **Tensegrity Module** comprises two subunits that, together, undergo zero net rotation (to first order) under a longitudinal (vertical in this view) load.

an increase in the rotation angle, but by virtue of the mirror arrangement, the net first-order rotation between the uppermost and lowermost planes is zero. The need to have zero net rotation between these planes under all loading conditions in a typical practical structure is what prompts the use of the mirror configuration. Force and moment loadings other than simple axial compression produce only second-order deformations through strains in the struts and cables.

Simple algebraic expressions have been derived to describe the deformations, under load, of multimodule platelike and mast structures, thereby making it possible

to design such structures without need for computers. Perhaps the most important rules for designing a tensegrity structure are that (1) the lengths of the struts and cables are critical and they determine the unloaded shape of the structure, but that (2) the preloads (discussed in the next paragraph) in the cables and struts determine the degree of rigidity under external load.

To make a module stowable, it is necessary to provide for disconnection of the ends of many of the struts and/or make the struts collapsible (e.g., telescoping). To make a module deployable, one must provide means to reconnect the struts if disconnected and re-extend them if collapsed. The means of deployment must include means to apply the required preloads to the cables and struts. In cases of manual stowage and deployment, such means can include toggles and turnbuckles. For automated deployment, more sophisticated means are needed. In the structure of Figure 2, the struts are telescoping piston/cylinder units that are extended pneumatically and locked at full extension by spring-loaded mechanisms.

*This work was done by Glenn W. Zeiders of the Sirius Group, Larry J. Bradford of CAT Flight Services, and Richard C. Cleve of Elk River Engineering for **Marshall Space Flight Center**. For further information, contact:*

*Glenn W. Zeiders  
Sirius Group  
2803 Downing Court  
Huntsville, AL 35801  
E-mail: gzeiders@knology.net  
Refer to MFS-31872.*





## Centrifugal Adsorption Cartridge System

Notable features include efficient collection of bioproducts and removal of bubbles.

Lyndon B. Johnson Space Center, Houston, Texas

The centrifugal adsorption cartridge system (CACS) is an apparatus that recovers one or more bioproduct(s) from a dilute aqueous solution or suspension flowing from a bioreactor. The CACS can be used both on Earth in unit gravity and in space in low gravity. The CACS can be connected downstream from the bioreactor; alternatively, it can be connected into a flow loop that includes the bioreactor so that the liquid can be recycled.

A centrifugal adsorption cartridge in the CACS (see figure) includes two concentric cylinders with a spiral ramp between them. The volume between the inner and outer cylinders, and between the turns of the spiral ramp is packed with an adsorbent material. The inner cylinder is a sieve tube covered with a gas-permeable, hydrophobic membrane.

During operation, the liquid effluent from the bioreactor is introduced at one end of the spiral ramp, which then constrains the liquid to flow along the spiral path through the adsorbent material. The spiral ramp also makes the flow more nearly uniform than it would otherwise be, and it minimizes any channeling other than that of the spiral flow itself.

The adsorbent material is formulated to selectively capture the bioproduct(s) of interest. The bioproduct(s) can then be stored in bound form in the cartridge or else eluted from the cartridge.

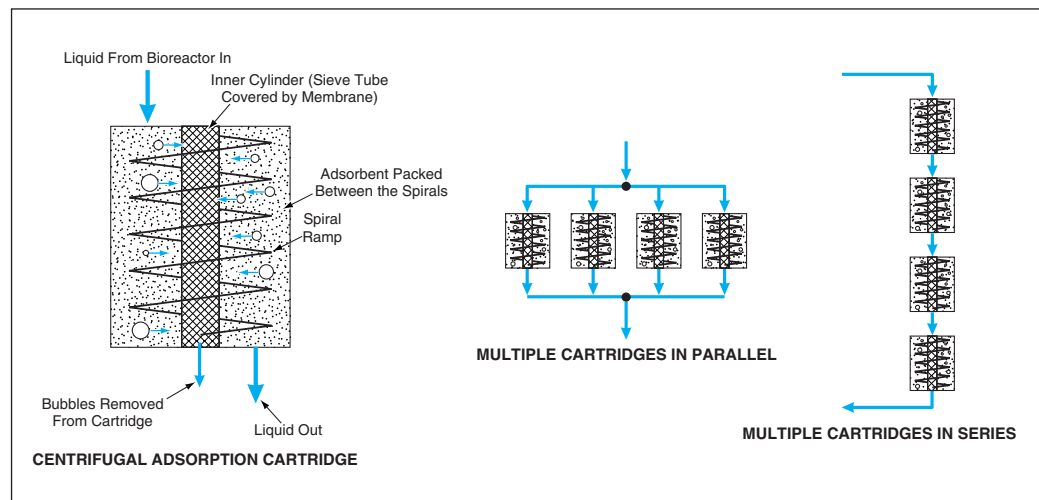
The centrifugal effect of the spiral flow is utilized to remove gas bubbles from the liquid. The centrifugal effect forces the bubbles radially inward, toward and through the membrane of the inner cylinder. The gas-permeable, hydrophobic membrane allows the bubbles to enter the inner cylinder while keeping the liquid out. The bubbles that thus enter the cylinder are vented to the atmosphere. The spacing between the ramps determines rate of flow along the spiral, and thereby affects the air-bubble-removal efficiency. The spacing between the ramps also determines the length of the fluid path through the cartridge adsorbent, and thus affects the bioproduct-capture efficiency of the cartridge.

Depending on the application, several cartridges could be connected in a

serial or parallel flow arrangement. A parallel arrangement can be used to increase product-capturing and flow capacities while maintaining a low pressure drop. A serial arrangement can be used to obtain high product-capturing capacity; alternatively, series-connected cartridges can be packed with different adsorbents to capture different bioproducts simultaneously.

*This work was done by Steve R. Gonda of Johnson Space Center and Yow-Min D. Tsao and Wenshan Lee of Wyle Laboratories.*

*This invention is owned by NASA, and a patent application has been filed. Inquiries concerning nonexclusive or exclusive license for its commercial development should be addressed to the Patent Counsel, Johnson Space Center, (281) 483-0837. Refer to MSC-22863.*



In a Centrifugal Adsorption Cartridge, the liquid effluent from a bioreactor is channeled along a spiral flow path through a selectively adsorbent material. The length of the spiral path contributes to efficient collection of a bioproduct suspended or dissolved in the liquid. Multiple centrifugal adsorption cartridges can be connected in series or parallel.

## Ultrasonic Apparatus for Pulverizing Brittle Material

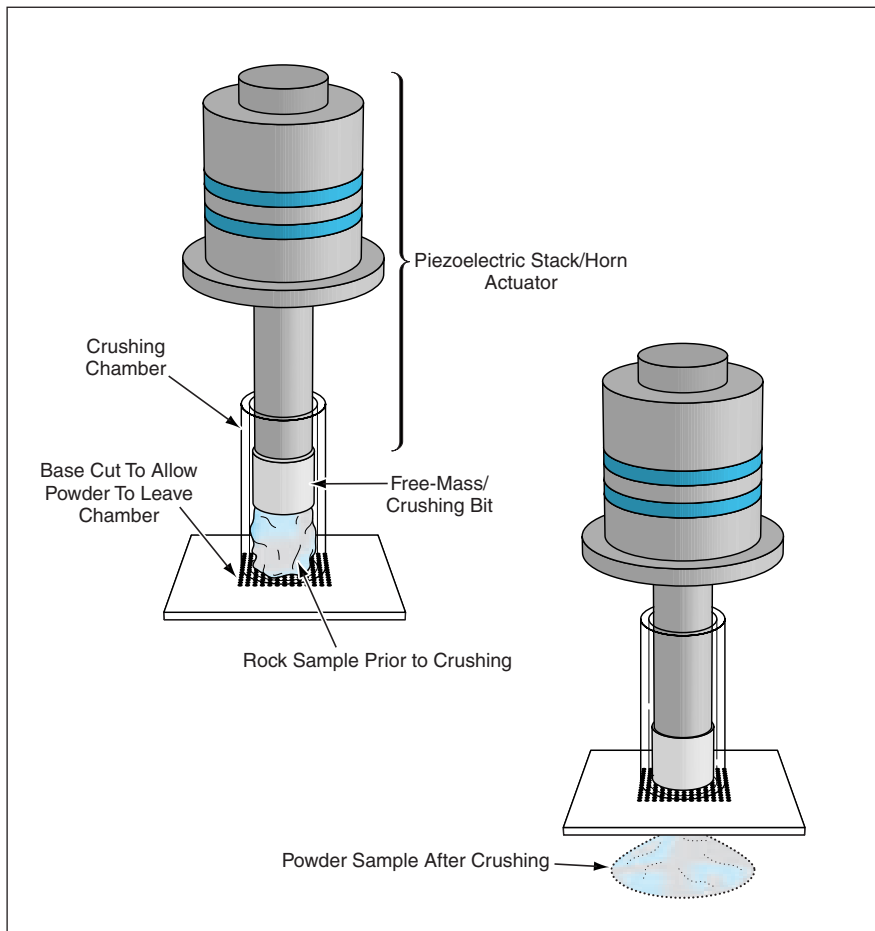
Characteristics include light weight, low preload, and low power demand.

NASA's Jet Propulsion Laboratory, Pasadena, California

The figure depicts an apparatus that pulverizes brittle material by means of a combination of ultrasonic and sonic vibration, hammering, and abrasion. The

basic design of the apparatus could be specialized to be a portable version for use by a geologist in collecting powdered rock samples for analysis in the

field or in a laboratory. Alternatively, a larger benchtop version could be designed for milling and mixing of precursor powders for such purposes as synthe-



Driven by the Piezoelectric Stack/Horn Actuator, the free-mass hammers the rock sample in the crushing chamber. Particles of rock leave the chamber through a sieve-covered hole at the bottom.

sis of ceramic and other polycrystalline materials or preparing powder samples for x-ray diffraction or x-ray fluorescence measurements to determine crystalline structures and compositions. Among the most attractive characteristics of this apparatus are its light weight

and the ability to function without need for a large preload or a large power supply: It has been estimated that a portable version could have a mass <0.5 kg, would consume less than 1 W·h of energy in milling a 1-cm<sup>3</sup> volume of rock, and could operate at a preload <10 N.

The basic design and principle of operation of this apparatus are similar to those of other apparatuses described in a series of prior *NASA Tech Briefs* articles, the two most relevant being “Ultrasonic/Sonic Drill/Corers With Integrated Sensors” (NPO-20856), Vol. 25, No. 1 (January 2001), page 38 and “Ultrasonic/Sonic Mechanisms for Deep Drilling and Coring” (NPO-30291), Vol. 27, No. 9 (September 2003), page 65. As before, vibrations are excited by means of a piezoelectric actuator, an ultrasonic horn, and a mass that is free to move axially over a limited range. As before, the ultrasonic harmonic motion of the horn drives the free-mass in a combination of ultrasonic harmonic and lower-frequency hammering motion.

In this case, the free-mass is confined within a hollow cylinder that serves as a crushing chamber, and the free-mass serves as a crushing or milling tool. The hammering of the free-mass against a material sample at the lower end of the chamber grinds the sample into powder in a relatively short time. The restriction of the free-mass to axial motion only makes the grinding very efficient. The free-mass can be fabricated to have teeth on its lower face to enhance the grinding effect. Optionally, there can be a hole at the bottom of the chamber covered with a sieve to tailor the size distribution of the powder leaving the crushing chamber.

*This work was done by Stewart Sherrit, Xiaohu Bao, Yoseph Bar-Cohen, Benjamin Dolgin, and Zensheu Chang of Caltech for NASA's Jet Propulsion Laboratory. Further information is contained in a TSP (see page 1).*

NPO-30682



## Transplanting Retinal Cells Using Bucky Paper for Support

Bucky paper supports the cells before, during, and after surgery.

*Ames Research Center, Moffett Field, California*

A novel treatment for retinal degenerative disorders involving transplantation of cells into the eye is currently under development at NASA Ames Research Center and Stanford University School of Medicine. The technique uses bucky paper as a support material for retinal pigment epithelial (RPE) cells, iris pigment epithelial (IPE) cells, and/or stem cells. This technology is envisioned as a treatment for age-related macular degeneration, which is the leading cause of blindness in persons over age 65 in Western nations. Additionally, patients with other retinal degenerative disorders, such as retinitis pigmentosa, may be treated by this strategy.

Bucky paper is a mesh of carbon nanotubes (CNTs), as shown in Figure 1, that can be made from any of the commercial sources of CNTs. Bucky paper is biocompatible and capable of supporting the growth of biological cells. Because bucky paper is highly porous, nutrients, oxygen, carbon dioxide, and waste can readily diffuse through it. The thickness, density, and porosity of bucky paper can be tailored in manufacturing. For transplantation of cells into the retina, bucky paper serves simultaneously as a substrate for cell growth and as a barrier for new blood vessel formation, which can be a problem in the exudative type of macular degeneration.

Bucky paper is easily handled during surgical implantation into the eye. Through appropriate choice of manufacturing processes, bucky paper can

be made relatively rigid yet able to conform to the retina when the bucky paper is implanted. Bucky paper offers a distinct advantage over other materials that have been investigated for retinal cell transplantation — lens capsule and Descemet's membrane — which are difficult to handle during

surgery because they are flimsy and do not stay flat.

In preparation for implantation, the selected cells are first cultured onto a piece of bucky paper. A retinotomy is then performed, the cell-covered bucky paper is implanted, and the retina is reattached. Because bucky paper does

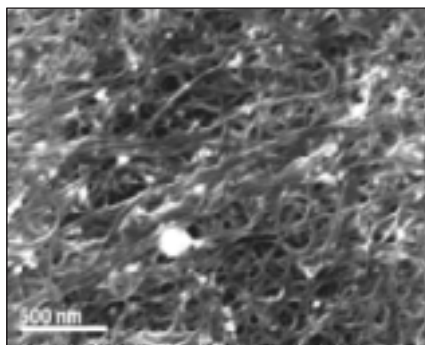


Figure 1. The Mesh of Carbon Nanotubes in Bucky Paper can be seen in this high magnification scanning electron micrograph .

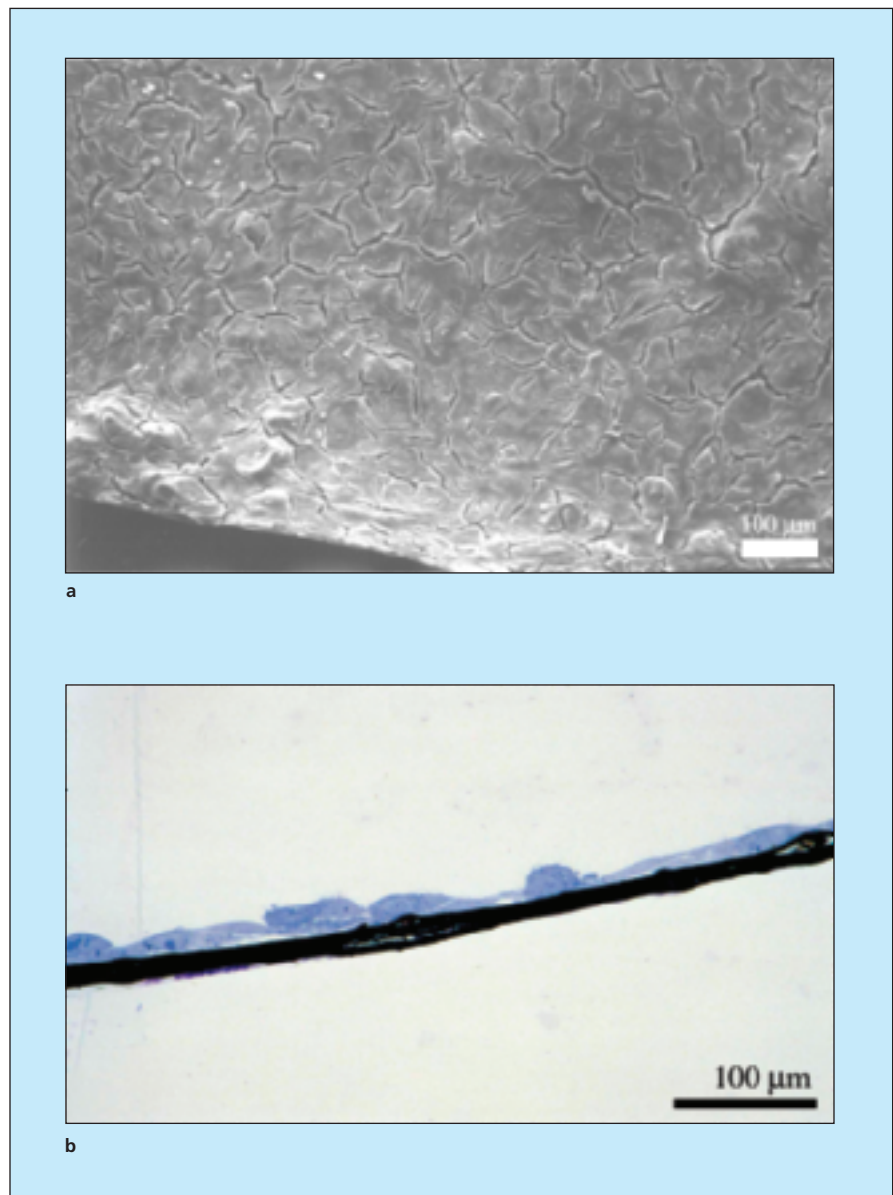


Figure 2. Micrographs of RPE Cells illustrate the following: (a) human RPE cells cultured on bucky paper, as shown in this scanning electron micrograph, form a monolayer which is suitable for transplantation into the retina and (b) light micrograph of human RPE cells (stained blue) cultured on bucky paper (black) viewed in cross section.

not trigger an inflammatory reaction in the eye, it can be left in place after transplantation to serve as a basement membrane patch.

The attachment of RPE (see Figure 2), IPE, and/or stem cells onto the bucky paper may be enhanced by chemically modifying or coating the bucky paper with one or more biologically active substances. The ability to easily

make these modifications may serve as an important way of optimizing retinal cell transplantation for macular degeneration and retinitis pigmentosa and may facilitate other ophthalmologic applications as well.

*This patent pending work was performed by David J. Loftus, Martin Cinke, and Meyya Meyyappan of Ames Research Center, Center for Nanotechnology, and by Har-*

*vey Fishman, Ted Leng, Philip Huie, and Kalayaan Bilbao of Stanford University School of Medicine, Department of Ophthalmology. Further information is contained in a TSP (see page 1).*

*Inquiries concerning rights for the commercial use of this invention should be addressed to the Patent Counsel, Ames Research Center, (650) 604-5104. Refer to ARC-14940.*

---

## Using an Ultrasonic Instrument to Size Extravascular Bubbles

Measurements could be used to guide prebreathing of oxygen to reduce the risk of decompression sickness.

*Lyndon B. Johnson Space Center, Houston, Texas*

In an ongoing development project, microscopic bubbles in extravascular tissue in a human body will be detected by use of an enhanced version of the apparatus described in "Ultrasonic Bubble-Sizing Instrument" (MSC-22980), *NASA Tech Briefs*, Vol. 24, No. 10 (October 2000), page 62. To recapitulate: The physical basis of the instrument is the use of ultrasound to excite and measure the resonant behavior (oscillatory expansion and contraction) of bubbles. The resonant behavior is a function of the bubble diameter; the instrument exploits the diameter dependence of the resonance frequency and the general nonlinearity of the ultrasonic response of bubbles to detect bubbles and potentially measure their diameters.

In the cited prior article, the application given most prominent mention was the measurement of gaseous emboli (es-

entially, gas bubbles in blood vessels) that cause decompression sickness and complications associated with cardiopulmonary surgery. According to the present proposal, the instrument capabilities would be extended to measure extravascular bubbles with diameters in the approximate range of 1 to 30  $\mu\text{m}$ .

The proposed use of the instrument could contribute further to the understanding and prevention of decompression sickness: There is evidence that suggests that prebreathing oxygen greatly reduces the risk of decompression sickness by reducing the number of microscopic extravascular bubbles. By using the ultrasonic bubble-sizing instrument to detect and/or measure the sizes of such bubbles, it might be possible to predict the risk of decompression sickness. The instrument also has potential as a tool to guide the oxygen-prebreathing

schedules of astronauts; high-altitude aviators; individuals who undertake high-altitude, low-opening (HALO) parachute jumps; and others at risk of decompression sickness. For example, an individual at serious risk of decompression sickness because of high concentrations of extravascular microscopic bubbles could be given a warning to continue to prebreathe oxygen until it was safe to decompress.

*This work was done by Patrick J. Magari, Robert J. Kline-Schoder, and Marc A. Kenton of Creare, Inc., for Johnson Space Center. For further information, contact:*

*Creare, Inc.  
P.O. Box 71  
Hanover, NH 03755  
Phone: (603) 643-3800  
Fax: (603) 643-4657  
E-mail: info@creare.com  
Refer to MSC-23128.*



## Coronagraphic Notch Filter for Raman Spectroscopy

Design could be optimized for attenuating pump light and transmitting Raman-scattered light.

NASA's Jet Propulsion Laboratory, Pasadena, California

A modified coronagraph has been proposed as a prototype of improved notch filters in Raman spectrometers. Coronagraphic notch filters could offer alternatives to both (1) the large and expensive double or triple monochromators in older Raman spectrometers and (2) holographic notch filters, which are less expensive but are subject to environmental degradation as well as to limitations of geometry and spectral range.

Measurement of a Raman spectrum is an exercise in measuring and resolving faint spectral lines close to a bright peak: In Raman spectroscopy, a monochromatic beam of light (the pump beam) excites a sample of material that one seeks to analyze. The pump beam generates a small flux of scattered light at wavelengths slightly greater than that of the pump beam. The shift in wavelength of the scattered light from the pump wavelength is known in the art as the Stokes shift. Typically, the flux of scattered light is of the order of  $10^{-7} \times$  that of the pump beam and the Stokes shift lies in the wave-number range of 100 to 3,000  $\text{cm}^{-1}$ . A notch filter can be used to suppress the pump-beam spectral peak while passing the nearby faint Raman spectral lines.

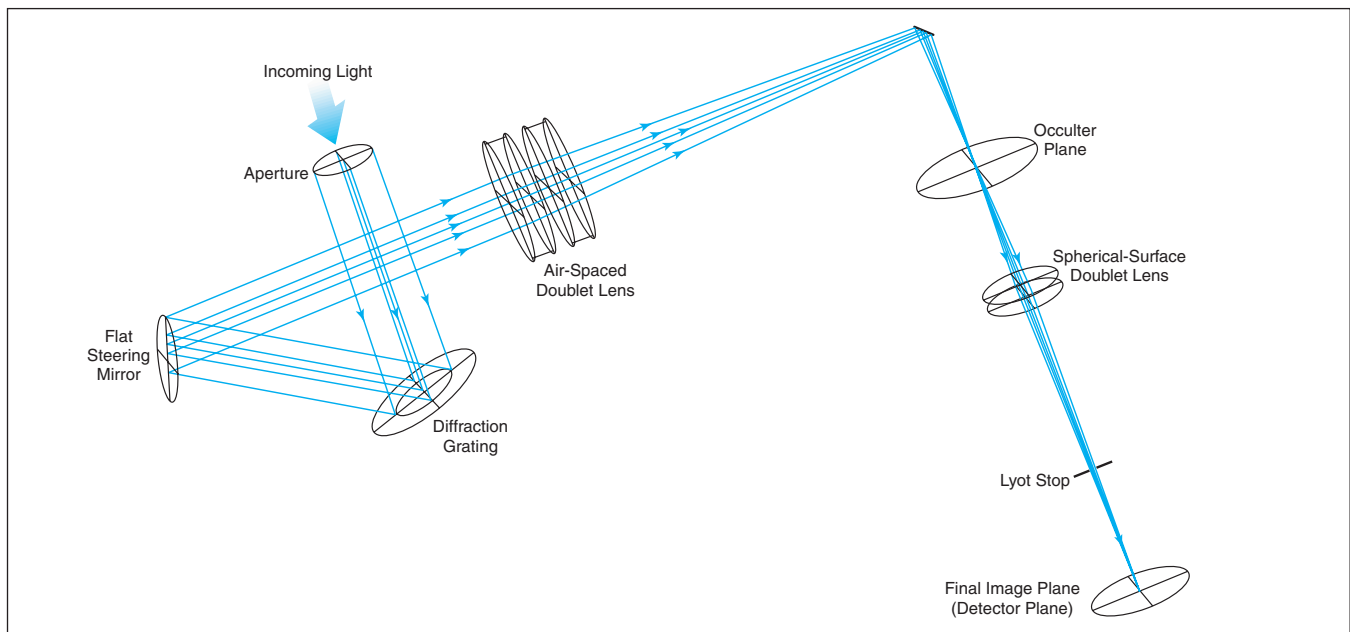
The basic principles of design and operation of a coronagraph offer an opportunity for engineering the spectral transmittance of the optics in a Raman spectrometer. A classical coronagraph may be understood as two imaging systems placed end to end, such that the first system forms an intermediate real image of a nominally infinitely distant object and the second system forms a final real image of the intermediate real image. If the light incident on the first telescope is collimated, then the intermediate image is a point-spread function (PSF). If an appropriately tailored occulting spot (e.g., a Gaussian-apodized spot with maximum absorption on axis) is placed on the intermediate image plane, then the instrument inhibits transmission of light from an on-axis source. However, the PSFs of off-axis light sources are formed off axis — that is, away from the occulting spot — so that they become refocused onto the final image plane.

A properly designed coronagraph utilizes the diffraction from the intermediate occulting spot. In the exit-pupil plane, this diffraction forms a well-defined ring image in the vicinity of the geometric

image of the exit pupil. By placing an aperture stop sized to block the passage of the diffracted light (such an aperture is known in the art as a Lyot stop) in the exit-pupil plane, it is possible, in principle, to obtain an extremely high rejection ratio.

While coronagraphs are not new, recent developments make it possible to enhance performance. One such development is that of the ability to write arbitrary absorption patterns on occulting spots at submicron resolution by use of electron-beam lithography. Another such development is that of superpolished optics.

One characteristic of a classical coronagraph essential to the proposed notch filter is that within the narrow typical Raman spectral range associated with a given pump laser line, the size of the PSF changes little with wavelength. However, the position of the PSF (in particular, its displacement from the occulting spot) can be made to vary considerably with wavelength by introducing a diffraction grating or other dispersive element into the optical train. Hence, one could obtain an extraordinarily sharp notch in the spectral transmittance of a coronagraphic filter by designing the dispersive element



A **Coronagraphic Filter** would include a modified coronagraph equipped with a diffraction grating and other components. The modification would be such as to optimize the functioning of the resulting instrument as a narrowband rejection (notch) filter.

and the other coronagraphic optics so that at the pump wavelength, the PSF is centered on the occulting spot.

The figure shows the optical layout according to one possible design of the proposed coronagraphic filter for a pump wavelength of 550 nm. The dispersive element would be a 500-line-per-millimeter diffraction grating, of which the first-order diffraction would be utilized. After passing through an aperture, the incoming light would strike the grating, followed by a flat steering mirror. An air-

spaced doublet lens incorporating an aspherical element would generate a PSF at the occulter (intermediate-image) plane. A spherical-surface doublet lens would reimage the light onto a detector plane. On its way to the detector plane, the light would pass through a Lyot stop. In principle, a linear array of photodetectors could be placed in the final image plane to measure the Raman spectrum. The depth of the notch at the pump wavelength, as well as other parameters of the performance of the coronagraphic filter,

could be tailored through the choice of the parameters of the optical components, including especially the dispersion of the grating; the aperture diameter, focal length, and aberrations of the first doublet lens; the length of the occulting spot along the axis of dispersion; and the diameter of the Lyot stop.

*This work was done by David Cohen and Robert Stürl of Caltech for NASA's Jet Propulsion Laboratory. Further information is contained in a TSP (see page 1). NPO-30504*

## On-the-Fly Mapping for Calibrating Directional Antennas

Source-size corrections are not necessary in this method.

NASA's Jet Propulsion Laboratory, Pasadena, California

An improved method of calibrating a large directional radio antenna of the type used in deep-space communication and radio astronomy has been developed. This method involves a raster-scanning-and-measurement technique denoted on-the-fly (OTF) mapping, applied in consideration of the results of a systematic analysis of the entire measurement procedure. Phenomena to which particular attention was paid in the analysis include (1) the noise characteristics of a total-power radiometer (TPR) that is used in the measurements and (2) troposphericly in-

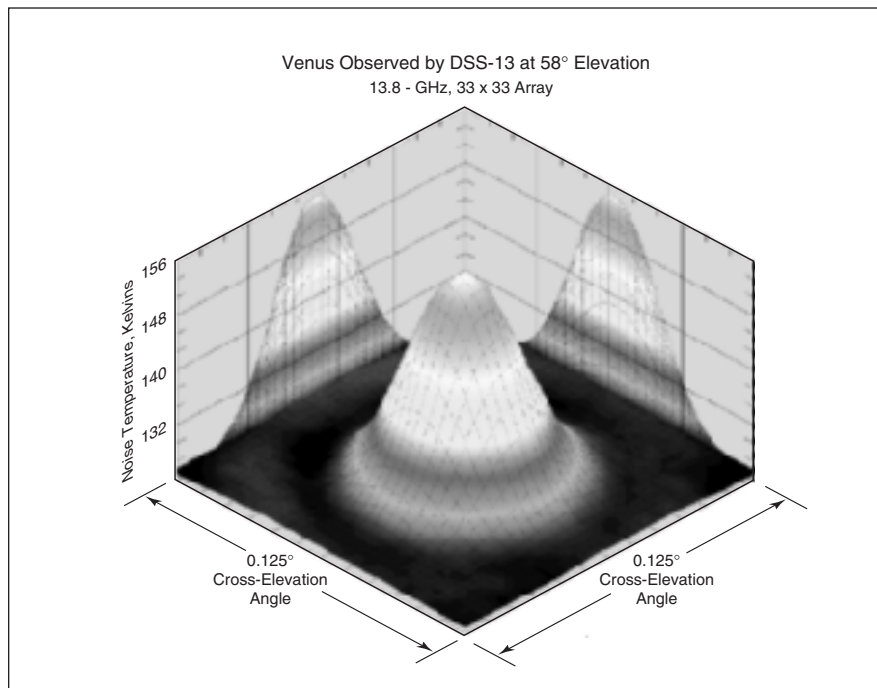
duced radiometer fluctuations. The method also involves the use of recently developed techniques for acquisition and reduction of data. In comparison with prior methods used to calibrate such antennas, this method yields an order-of-magnitude improvement in the precision of determinations of antenna aperture efficiency, and improvement by a factor of five or more in the precision of determination of pointing error and beam width.

Prerequisite to a meaningful description of the present method is some background information concerning three aspects of

the problem of calibrating an antenna of the type in question:

- In OTF mapping measurements in which a TPR is used, the desired data are the peak temperature corresponding to a radio source, the pointing offset when the antenna is commanded to point toward the source, and the shape of the main lobe of the antenna beam, all as functions of the antenna beam elevation and azimuth angles. These data enable one to calculate the (1) antenna aperture efficiency by comparing the measured peak temperature with that expected for a 100-percent-efficient antenna, (2) the mechanical pointing error resulting from small misalignments of various parts of the antenna structure, and (3) misalignments of the antenna subreflector and other mirrors.
- For practical reasons having to do with obtaining adequate angular resolution and all-sky coverage, it is necessary to perform azimuth and elevation scans fairly rapidly.
- Many natural radio sources used in calibrating antennas are only approximately pointlike: some sources subtend angles greater than the beam width of a given antenna. In such a case, the antenna partially resolves the source structure and does not collect all of the radiation emitted by the source. This makes it necessary to estimate how much of the total known radiation from the source would actually be collected by the antenna if it were 100-percent efficient. The resulting estimate, leading to a source-size correction factor, introduces another degree of uncertainty to the measurements. OTF mapping can remove this uncertainty.

The key to using OTF mapping to solve all three aspects of the calibration problem



The TPR Readout Data plotted here were acquired in a test raster scan of a portion of the sky, near an elevation angle of 58°, that contained the planet Venus when it was relatively close to Earth. The horizontal axes on this plot correspond to elevation and cross-elevation angles. The vertical axis represents noise temperature in Kelvins.

is to maintain a constant, known angular velocity when scanning the antenna along a given direction. To ensure alignment of the individual subscans within the full raster, the angular position of the first data point of each subscan is determined from readings of azimuth- and elevation-angle encoders, while the angular positions of the rest of the subscan data points are determined by timing at the constant angular velocity. Hence, if the TPR reading is sampled at a constant known rate, then the relative angular position at which each datum is taken is known with high accuracy, and antenna-settling time is no longer an issue. The data-acquisition algorithms used in

OTF mapping provide for computation of the angular positions of radio sources, such that at any given time, the position of the antenna relative to a source is known.

The acquisition of data in the OTF mode necessarily entails attenuation of high-frequency information as a consequence of the integration that occurs during the sampling intervals. The high-frequency information can be recovered in an inverse-filtering computation.

Even though the antenna beam does not sample all of the radiation from an extended radio source at a given instant, the completed raster scan does cover the entire solid angle subtended by the source and,

hence contains a sampling of all the radiation from that source. Consequently, no source-size correction is necessary in OTF mapping. The resulting set of data registered on a two-dimensional field of sampling points (see figure) can be used to determine a least-squares-best-fit main beam pattern. The calibration parameters can then be determined from the main beam pattern.

*This work was done by David Rochblatt, Paul Richter, and Philip Withington of Caltech for NASA's Jet Propulsion Laboratory. Further information is contained in a TSP (see page 1). NPO-30648*

---

## Working Fluids for Increasing Capacities of Heat Pipes

**Fluids are formulated to make surface tensions increase with temperature.**

*John H. Glenn Research Center, Cleveland, Ohio*

A theoretical and experimental investigation has shown that the capacities of heat pipes can be increased through suitable reformulation of their working fluids. The surface tensions of all of the working fluids heretofore used in heat pipes decrease with temperature. As explained in more detail below, the limits on the performance of a heat pipe are associated with the decrease in the surface tension of the working fluid with temperature, and so one can enhance performance by reformulating the working fluid so that its surface tension increases with temperature. This improvement is applicable to almost any kind of heat pipe in almost any environment.

The heat-transfer capacity of a heat pipe in its normal operating-temperature range is subject to a capillary limit and a boiling limit. Both of these limits are associated with the temperature dependence of surface tension of the working

fluid. In the case of a traditional working fluid, the decrease in surface tension with temperature causes a body of the liquid phase of the working fluid to move toward a region of lower temperature, thus preventing the desired spreading of the liquid in the heated portion of the heat pipe. As a result, the available capillary-pressure pumping head decreases as the temperature of the evaporator end of the heat pipe increases, and operation becomes unstable.

Water has widely been used as a working fluid in heat pipes. Because the surface tension of water decreases with increasing temperature, the heat loads and other aspects of performance of heat pipes that contain water are limited. Dilute aqueous solutions of long-chain alcohols have shown promise as substitutes for water that can offer improved performance, because these solutions exhibit unusual surface-tension characteristics: Experiments have

shown that in the cases of an aqueous solution of an alcohol, the molecules of which contain chains of more than four carbon atoms, the surface tension increases with temperature when the temperature exceeds a certain value.

There are also other liquids that have surface tensions that increase with temperature and could be used as working fluids in heat pipes. For example, as a substitute for ammonia, which is the working fluid in some heat pipes, one could use a solution of ammonia and an ionic surfactant.

*This work was done by David F. Chao of Glenn Research Center and Nengli Zhang of Ohio Aerospace Institute. Further information is contained in a TSP (see page 1).*

*Inquiries concerning rights for the commercial use of this invention should be addressed to NASA Glenn Research Center, Commercial Technology Office, Attn: Steve Fedor, Mail Stop 4-8, 21000 Brookpark Road, Cleveland Ohio 44135. Refer to LEW-17270.*



## Σ **Computationally-Efficient Minimum-Time Aircraft Routes in the Presence of Winds**

**Minimum-time routes are achieved using 10 times less computational effort.**

*Ames Research Center, Moffett Field, California*

A computationally efficient algorithm for minimizing the flight time of an aircraft in a variable wind field has been invented. The algorithm, referred to as Neighboring Optimal Wind Routing (NOWR), is based upon neighboring-optimal-control (NOC) concepts and achieves minimum-time paths by adjusting aircraft heading according to wind conditions at an arbitrary number of wind measurement points along the flight route. The NOWR algorithm may either be used in a fast-time mode to compute minimum-time routes prior to flight, or may be used in a feedback mode to adjust aircraft heading in real-time. By traveling minimum-time routes instead of direct great-circle (direct) routes, flights across the United States can save an average of about 7 minutes, and as much as one hour of flight time during periods of strong jet-stream winds. The neighboring optimal routes computed via the NOWR technique have been shown to be within 1.5 percent of the absolute minimum-time routes for flights across the continental United States. On a typical 450-MHz Sun Ultra workstation, the NOWR algorithm produces complete minimum-time routes in less than 40 milliseconds. This corresponds to a rate of 25 optimal routes per second. The closest comparable optimization technique runs approximately 10 times slower.

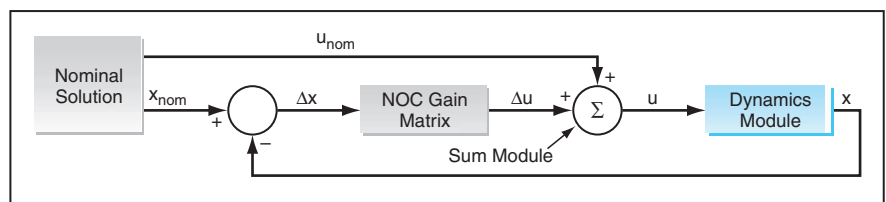
Airlines currently use various trial-and-error search techniques to determine which of a set of commonly traveled routes will minimize flight time. These algorithms are too computationally expensive for use in real-time systems, or in systems where many optimal routes need to be computed in a short amount of time. Instead of operating in real-time, airlines will typically plan a trajectory several hours in advance using wind forecasts. If winds change significantly from forecasts, the resulting flights will no longer be minimum-time. The need for a computationally

efficient wind-optimal routing algorithm is even greater in the case of new air-traffic-control automation concepts. For air-traffic-control automation, thousands of wind-optimal routes may need to be computed and checked for conflicts in just a few minutes. These factors motivated the need for a more efficient wind-optimal routing algorithm.

The NOWR algorithm is a special type of perturbation feedback control as shown in the figure. The nominal winds are modeled as system states, and are considered to be zero magnitude so that the nominal trajectory solution is simply a great-circle route between origin and destination. The actual winds are input as perturbations to the nominal winds, multiplied by time-varying NOWR gains, and then fed back as heading command perturbations to achieve a minimum-

time trajectory solution. The NOWR gains are computed using techniques from the calculus of variations. Because the nominal route is a great circle, and because the nominal winds are zero magnitude, the NOWR feedback gains may be normalized and applied to flights at any airspeed between any origin and destination using coordinate rotations and simple time and distance scaling. This one-solution-fits-all aspect of NOWR makes it a very powerful and practical technique.

The implementation procedure for NOWR is to either run a fast-time simulation to compute an optimal wind route, which can then be used as the basis for a filed flight plan, or one may use NOWR in real-time to achieve wind-optimal routes in a future free flight environment.



**Feedforward and Feedback** quantities are computed in an NOC approach to adjustment of control variables for optimization of the route taken by an aircraft.

The optimization process begins by first rotating coordinates so that the origin and destination points appear to be located along the equator of the rotated coordinate system. The distance unit is then scaled such that the distance from origin to destination is unity. The time unit is similarly scaled such that the airspeed of the aircraft is also unity. Because of this scaling, any flight between any two points appears to be mathematically similar. The winds along the flight route are then obtained from the Rapid Update Cycle (RUC), a national gridded wind system developed at the National Oceanic and

Atmospheric Administration. The NOWR algorithm may be adapted to use as many wind measurement points along the route as are desired, but in practice, about 10 or 15 points are sufficient. At each of these points, the predicted winds are multiplied by the NOWR gains to determine the optimal heading angles the aircraft should use to fly a minimum-time route. Once the optimal heading and the coordinates of the minimum-time route have been computed in the normalized coordinate system, the solution may be transformed back to real Earth coordinates through the inverse rotation equations.

The reason why this perturbation scheme is so efficient is that it is a simple linear feedback algorithm involving just a few algebraic steps. The excellent performance of NOWR in practice is achieved because winds typically vary in a smooth manner and do not contain many sharp nonlinearities or discontinuities.

*This work was done by Matthew R. Jardin of **Ames Research Center**. Further information is contained in a TSP (see page 1).*

*Inquiries concerning rights for the commercial use of this invention should be addressed to the Patent Counsel, Ames Research Center, (650) 604-5104. Refer to ARC-14554.*



### ⚙️ **Liquid-Metal-Fed Pulsed Plasma Thrusters**

A short document proposes liquid-metal-fed pulsed plasma thrusters for small spacecraft. The propellant liquid for such a thruster would be a low-melting-temperature metal that would be stored molten in an unpressurized, heated reservoir and would be pumped to the thruster by a magnetohydrodynamic coupler. The liquid would enter the thruster via a metal tube inside an electrically insulating ceramic tube. A capacitor would be connected between the outlet of the metal tube and the outer electrode of the thruster. The pumping would cause a drop of liquid to form at the outlet, eventually growing large enough to make contact with the outer electrode. Contact would close the circuit through the capacitor, causing the capacitor to discharge through the drop. The capacitor would have been charged with enough energy that the discharge would vaporize, ionize, and electromagnetically accelerate the contents of the metal drop. The resulting plasma would be ejected at a speed of about 50 km/s. The vaporization of the drop would reopen the circuit through the capacitor, enabling recharging of the capacitor. As pumping continued, a new drop would grow and the process would repeat.

*This work was done by Thomas Markusic of Marshall Space Flight Center. For further information, contact Brian Johnson, MSFC Commercialization Assistance Lead, at (256) 544-3518, [brian.s.johnson@nasa.gov](mailto:brian.s.johnson@nasa.gov), or access the Technical Support Package (TSP) (see page 1).  
MFS-31962*

### 📦 **Personal Radiation Protection System**

A report describes the personal radiation protection system (PRPS), which has been invented for use on the International Space Station and other spacecraft. The PRPS comprises walls that can be erected inside spacecraft, where and when needed, to reduce the amount of radiation to which personnel are exposed. The basic structural modules of the PRPS are pairs of 1-in. (2.54-cm)-thick plates of high-density polyethylene equipped with fasteners. The plates of each module are assembled with a lap joint. The modules are denoted bricks because they are designed to be stacked with overlaps, in a manner reminiscent of bricks, to build 2-in. (5.08-cm)-thick walls of various lengths and widths. The bricks are of two varieties: one for flat wall areas and one for corners. The corner bricks are specialized adaptations of the flat-area bricks that make it possible to join walls perpendicular to each other. Bricks are attached to spacecraft structures and to each other by use of straps that can be tightened to increase the strengths and stiffnesses of joints.

*This work was done by Mark McDonald of Johnson Space Center and Victoria Vinci of Johnson Engineering Corp. For further information, contact:*

*Johnson Engineering Corp.  
18100 Upper Bay Road, Suite 220  
Houston, TX 77058-3547  
Telephone No.: (281) 333-9729  
Refer to MSC-23330.*

### ⚙️ **Attitude Control for a Solar-Sail Spacecraft**

A report discusses the attitude-control system of a proposed spacecraft that would derive at least part of its propulsion from a solar sail. The spacecraft would include a bus module containing three or more reaction wheels, a boom attached at one end to the bus module and attached at its other end to a two-degree-of-freedom (DOF) gimbal at the nominal center of mass of a sail module. Each DOF of the gimbal could be independently locked against rotation or allowed to rotate freely. By using the reaction wheels to rotate the bus when at least one gimbal DOF was in the free state, the center of mass (CM) of the spacecraft could be shifted relative to the center of pressure (CP) on the solar sail. The resulting offset between the CM and CP would result in a solar torque, which could be used to change the attitude of the spacecraft. The report discusses numerous aspects of the dynamics and kinematics of the spacecraft, along with the relationships between these aspects and the designs of such attitude-control-system components as sensors, motors, brakes, clutches, and gimbals.

*This work was done by Edward Mettler and Scott Ploen of Caltech for NASA's Jet Propulsion Laboratory. Further information is contained in a TSP (see page 1).  
NPO-30522*







National Aeronautics and  
Space Administration